

---

# A Contour Stochastic Gradient Langevin Dynamics Algorithm for Simulations of Multi-modal Distributions

---

**Wei Deng**  
Department of Mathematics  
Purdue University  
West Lafayette, IN, USA  
weideng056@gmail.com

**Guang Lin**  
Departments of Mathematics &  
School of Mechanical Engineering  
Purdue University  
West Lafayette, IN, USA  
guanglin@purdue.edu

**Faming Liang\***  
Departments of Statistics  
Purdue University  
West Lafayette, IN, USA  
fmliang@purdue.edu

## Abstract

We propose an adaptively weighted stochastic gradient Langevin dynamics algorithm (SGLD), so-called contour stochastic gradient Langevin dynamics (CSGLD), for Bayesian learning in big data statistics. The proposed algorithm is essentially a *scalable dynamic importance sampler*, which automatically *flattens* the target distribution such that the simulation for a multi-modal distribution can be greatly facilitated. Theoretically, we prove a stability condition and establish the asymptotic convergence of the self-adapting parameter to a *unique fixed-point*, regardless of the non-convexity of the original energy function; we also present an error analysis for the weighted averaging estimators. Empirically, the CSGLD algorithm is tested on multiple benchmark datasets including CIFAR10 and CIFAR100. The numerical results indicate its superiority to avoid the local trap problem in training deep neural networks.

## 1 Introduction

AI safety has long been an important issue in the deep learning community. A promising solution to the problem is Markov chain Monte Carlo (MCMC), which leads to asymptotically correct uncertainty quantification for deep neural network (DNN) models. However, traditional MCMC algorithms [Metropolis et al., 1953, Hastings, 1970] are not scalable to big datasets that deep learning models rely on, although they have achieved significant successes in many scientific areas such as statistical physics and bioinformatics. It was not until the study of stochastic gradient Langevin dynamics (SGLD) [Welling and Teh, 2011] that resolves the scalability issue encountered in Monte Carlo computing for big data problems. Ever since, a variety of scalable stochastic gradient Markov chain Monte Carlo (SGMCMC) algorithms have been developed based on strategies such as Hamiltonian dynamics [Chen et al., 2014, Ma et al., 2015, Ding et al., 2014], Hessian approximation [Ahn et al., 2012, Li et al., 2016, Şimşekli et al., 2016], and higher-order numerical schemes [Chen et al., 2015, Li et al., 2019]. Despite their theoretical guarantees in statistical inference [Chen et al., 2015, Teh et al., 2016, Vollmer et al., 2016] and non-convex optimization [Zhang et al., 2017, Raginsky et al., 2017, Xu et al., 2018], these algorithms often converge slowly, which makes them hard to be used for efficient uncertainty quantification for many AI safety problems.

To develop more efficient SGMCMC algorithms, we seek inspirations from traditional MCMC algorithms, such as simulated annealing [Kirkpatrick et al., 1983], parallel tempering [Swendsen and Wang, 1986, Geyer, 1991], and flat histogram algorithms [Berg and Neuhaus, 1991, Wang and Landau,

---

\*To whom correspondence should be addressed: Faming Liang.

2001]. In particular, simulated annealing proposes to decay temperatures to increase the hitting probability to the global optima [Mangoubi and Vishnoi, 2018], which, however, often gets stuck into a local optimum with a fast cooling schedule. Parallel tempering proposes to swap positions of neighboring Markov chains according to an acceptance-rejection rule. However, under the mini-batch setting, it often requires a large correction which is known to deteriorate its performance [Deng et al., 2020]. The flat histogram algorithms, such as the multicanonical [Berg and Neuhaus, 1991] and Wang-Landau [Wang and Landau, 2001] algorithms, were first proposed to sample discrete states of Ising models by yielding a flat histogram in the energy space, and then extended as a general dynamic importance sampling algorithm, the so-called stochastic approximation Monte Carlo (SAMC) algorithm [Liang, 2005, Liang et al., 2007, Liang, 2009]. Theoretical studies [Lelièvre et al., 2008, Liang, 2010, Fort et al., 2015] support the efficiency of the flat histogram algorithms in Monte Carlo computing for small data problems. However, it is still unclear how to adapt the flat histogram idea to accelerate the convergence of SGMCMC, ensuring efficient uncertainty quantification for AI safety problems.

This paper proposes the so-called contour stochastic gradient Langevin dynamics (CSGLD) algorithm, which successfully extends the flat histogram idea to SGMCMC. Like the SAMC algorithm [Liang, 2005, Liang et al., 2007, Liang, 2009], CSGLD works as a dynamic importance sampling algorithm, which adaptively adjusts the target measure at each iteration and accounts for the bias introduced thereby by importance weights. However, theoretical analysis for the two types of dynamic importance sampling algorithms can be quite different due to the fundamental difference in their transition kernels. We proceed by justifying the stability condition for CSGLD based on the perturbation theory, and establishing ergodicity of CSGLD based on newly developed theory for the convergence of adaptive SGLD. Empirically, we test the performance of CSGLD through a few experiments. It achieves remarkable performance on some synthetic data, UCI datasets, and computer vision datasets such as CIFAR10 and CIFAR100.

## 2 Contour stochastic gradient Langevin dynamics

Suppose we are interested in sampling from a probability measure  $\pi(\mathbf{x})$  with the density given by

$$\pi(\mathbf{x}) \propto \exp(-U(\mathbf{x})/\tau), \quad \mathbf{x} \in \mathcal{X}, \quad (1)$$

where  $\mathcal{X}$  denotes the sample space,  $U(\mathbf{x})$  is the energy function, and  $\tau$  is the temperature. It is known that when  $U(\mathbf{x})$  is highly non-convex, SGLD can mix very slowly [Raginsky et al., 2017]. To accelerate the convergence, we exploit the flat histogram idea in SGLD.

Suppose that we have partitioned the sample space  $\mathcal{X}$  into  $m$  subregions based on the energy function  $U(\mathbf{x})$ :  $\mathcal{X}_1 = \{\mathbf{x} : U(\mathbf{x}) \leq u_1\}$ ,  $\mathcal{X}_2 = \{\mathbf{x} : u_1 < U(\mathbf{x}) \leq u_2\}$ ,  $\dots$ ,  $\mathcal{X}_{m-1} = \{\mathbf{x} : u_{m-2} < U(\mathbf{x}) \leq u_{m-1}\}$ , and  $\mathcal{X}_m = \{\mathbf{x} : U(\mathbf{x}) > u_{m-1}\}$ , where  $-\infty < u_1 < u_2 < \dots < u_{m-1} < \infty$  are specified by the user. For convenience, we set  $u_0 = -\infty$  and  $u_m = \infty$ . Without loss of generality, we assume  $u_{i+1} - u_i = \Delta u$  for  $i = 1, \dots, m-2$ . We propose to simulate from a flattened density

$$\varpi_{\Psi_{\theta}}(\mathbf{x}) \propto \frac{\pi(\mathbf{x})}{\Psi_{\theta}^{\zeta}(U(\mathbf{x}))}, \quad (2)$$

where  $\zeta > 0$  is a hyperparameter controlling the geometric property of the flattened density (see Figure 1(a) for illustration), and  $\theta = (\theta(1), \theta(2), \dots, \theta(m))$  is an unknown vector taking values in the space:

$$\Theta = \left\{ (\theta(1), \theta(2), \dots, \theta(m)) \mid 0 < \theta(1), \theta(2), \dots, \theta(m) < 1 \text{ and } \sum_{i=1}^m \theta(i) = 1 \right\}. \quad (3)$$

### 2.1 A naïve contour SGLD

It is known if we set <sup>†</sup>

$$\begin{aligned} \text{(i)} \quad & \zeta = 1 \text{ and } \Psi_{\theta}(U(\mathbf{x})) = \sum_{i=1}^m \theta(i) 1_{u_{i-1} < U(\mathbf{x}) \leq u_i}, \\ \text{(ii)} \quad & \theta(i) = \theta_{\star}(i), \text{ where } \theta_{\star}(i) = \int_{\mathcal{X}_i} \pi(\mathbf{x}) d\mathbf{x} \text{ for } i \in \{1, 2, \dots, m\}, \end{aligned} \quad (4)$$

<sup>†</sup> $1_A$  is an indicator function that takes value 1 if event  $A$  occurs and 0 otherwise.

the algorithm will act like the SAMC algorithm [Liang et al., 2007], yielding a flat histogram in the space of energy (see the pink curve in Figure 1(b)). Theoretically, such a density flattening strategy enables a sharper logarithmic Sobolev inequality and accelerates the convergence of simulations [Lelièvre et al., 2008, Fort et al., 2015]. However, such a density flattening setting only works under the framework of the Metropolis algorithm [Metropolis et al., 1953]. A naïve application of the step function in formula (4(i)) to SGLD results in  $\frac{\partial \log \Psi_\theta(u)}{\partial u} = \frac{1}{\Psi_\theta(u)} \frac{\partial \Psi_\theta(u)}{\partial u} = 0$  almost everywhere, which leads to the *vanishing-gradient problem* for SGLD. Calculating the gradient for the naïve contour SGLD, we have

$$\nabla_x \log \varpi_{\Psi_\theta}(x) = - \left[ 1 + \zeta \tau \frac{\partial \log \Psi_\theta(u)}{\partial u} \right] \frac{\nabla_x U(x)}{\tau} = - \frac{\nabla_x U(x)}{\tau}.$$

As such, the naïve algorithm behaves like SGLD and fails to simulate from the flattened density (2).

## 2.2 How to resolve the vanishing gradient

To tackle this issue, we propose to set  $\Psi_\theta(u)$  as a piecewise continuous function:

$$\Psi_\theta(u) = \sum_{i=1}^m \left( \theta(i-1) e^{(\log \theta(i) - \log \theta(i-1)) \frac{u - u_{i-1}}{\Delta u}} \right) 1_{u_{i-1} < u \leq u_i}, \quad (5)$$

where  $\theta(0)$  is fixed to  $\theta(1)$  for simplicity. A direct calculation shows that

$$\begin{aligned} \nabla_x \log \varpi_{\Psi_\theta}(\mathbf{x}) &= - \left[ 1 + \zeta \tau \frac{\partial \log \Psi_\theta(u)}{\partial u} \right] \frac{\nabla_x U(\mathbf{x})}{\tau} \\ &= - \left[ 1 + \zeta \tau \frac{\log \theta(J(\mathbf{x})) - \log \theta((J(\mathbf{x}) - 1) \vee 1)}{\Delta u} \right] \frac{\nabla_x U(\mathbf{x})}{\tau}, \end{aligned} \quad (6)$$

where  $J(\mathbf{x}) \in \{1, 2, \dots, m\}$  denotes the index that  $\mathbf{x}$  belongs to, i.e.,  $u_{J(\mathbf{x})-1} < U(\mathbf{x}) \leq u_{J(\mathbf{x})}$ .<sup>§</sup>

## 2.3 Estimation via stochastic approximation

Since  $\theta_*$  is unknown, we propose to estimate it on the fly under the framework of stochastic approximation [Robbins and Monro, 1951]. Provided that a scalable transition kernel  $\Pi_{\theta_k}(\mathbf{x}_k, \cdot)$  is available and the energy function  $U(\mathbf{x})$  on the full data can be efficiently evaluated, the weighted density  $\varpi_{\Psi_\theta}(\mathbf{x})$  can be simulated by iterating between the following steps:

- (i) Simulate  $\mathbf{x}_{k+1}$  from  $\Pi_{\theta_k}(\mathbf{x}_k, \cdot)$ , which admits  $\varpi_{\theta_k}(\mathbf{x})$  as the invariant distribution,
- (ii)  $\theta_{k+1}(i) = \theta_k(i) + \omega_{k+1} \theta_k^\zeta(J(\mathbf{x}_{k+1})) (1_{i=J(\mathbf{x}_{k+1})} - \theta_k(i))$  for  $i \in \{1, 2, \dots, m\}$ .

where  $\theta_k$  denotes a working estimate of  $\theta$  at the  $k$ -th iteration. We expect that in a long run, such an algorithm can achieve an *optimization-sampling equilibrium* such that  $\theta_k$  converges to the fixed point  $\theta_*$  and the random vector  $\mathbf{x}_k$  converges weakly to the distribution  $\varpi_{\Psi_{\theta_*}}(\mathbf{x})$ .

To make the algorithm scalable to big data, we adopt the Langevin transition kernel for drawing samples at each iteration, for which a mini-batch of data can be used to accelerate computation. In addition, evaluating the energy  $U(\mathbf{x})$  on the full data can be quite expensive, while it is free to obtain the stochastic energy  $\tilde{U}(\mathbf{x})$  in evaluating the stochastic gradient  $\nabla_x \tilde{U}(\mathbf{x})$  due to the nature of auto-differentiation [Paszke et al., 2017]. For this reason, we propose a stochastic index  $J_{\tilde{U}}(\mathbf{x})$

$$J_{\tilde{U}}(\mathbf{x}) = \sum_{i=1}^m i 1_{u_{i-1} < \frac{N}{n} \tilde{U}(\mathbf{x}) \leq u_i}, \quad (8)$$

where  $N$  is the sample size of the full dataset and  $n$  is the mini-batch size. Let  $\{\epsilon_k\}_{k=1}^\infty$  and  $\{\omega_k\}_{k=1}^\infty$  denote the learning rates and step sizes for SGLD and stochastic approximation, respectively. Given the above notations, the proposed algorithm can be presented in Algorithm 1, which can be viewed as a *scalable Wang-Landau algorithm* for deep learning and big data problems.

## 2.4 Related work

Compared to the existing MCMC algorithms, the proposed algorithm has a few innovations:

<sup>§</sup>Eq.(6) shows a practical numerical scheme. An alternative is presented in the supplementary material.

---

**Algorithm 1** Contour SGLD Algorithm. One can conduct a resampling step from the pool of importance samples according to the importance weights to obtain the original distribution. For more scalable updates, one can adopt the stochastic approximation scheme Eq.(15) in Deng et al. [2022].

---

- [1.] (**Data subsampling**) Simulate a mini-batch of data of size  $n$  from the whole dataset of size  $N$ ; Compute the stochastic gradient  $\nabla_{\mathbf{x}} \tilde{U}(\mathbf{x}_k)$  and stochastic energy  $\tilde{U}(\mathbf{x}_k)$ .  
 [2.] (**Simulation step**) Sample  $\mathbf{x}_{k+1}$  using the SGLD algorithm based on  $\mathbf{x}_k$  and  $\boldsymbol{\theta}_k$ , i.e.,

$$\mathbf{x}_{k+1} = \mathbf{x}_k - \epsilon_{k+1} \frac{N}{n} \underbrace{\left[ 1 + \zeta \tau \frac{\log \theta_k(J_{\tilde{U}}(\mathbf{x}_k)) - \log \theta_k((J_{\tilde{U}}(\mathbf{x}_k) - 1) \vee 1)}{\Delta u} \right]}_{\text{gradient multiplier}} \nabla_{\mathbf{x}} \tilde{U}(\mathbf{x}_k) + \sqrt{2\tau\epsilon_{k+1}} \mathbf{w}_{k+1}, \quad (9)$$

where  $\mathbf{w}_{k+1} \sim N(0, \mathbf{I}_d)$ ,  $d$  is the dimension,  $\epsilon_{k+1}$  is the learning rate, and  $\tau$  is the temperature.

- [3.] (**Stochastic approximation**) Update the estimate of  $\theta(i)$ 's for  $i = 1, 2, \dots, m$  by setting

$$\theta_{k+1}(i) = \theta_k(i) + \omega_{k+1} \theta_k^\zeta(J_{\tilde{U}}(\mathbf{x}_{k+1})) \left( 1_{i=J_{\tilde{U}}(\mathbf{x}_{k+1})} - \theta_k(i) \right), \quad (10)$$

where  $1_{i=J_{\tilde{U}}(\mathbf{x}_{k+1})}$  is an indicator function which equals 1 if  $i = J_{\tilde{U}}(\mathbf{x}_{k+1})$  and 0 otherwise.

---

First, CSGLD is an adaptive MCMC algorithm based on the *Langevin transition kernel* instead of the *Metropolis transition kernel* [Liang et al., 2007, Fort et al., 2015]. As a result, the existing convergence theory for the Wang-Landau algorithm does not apply. To resolve this issue, we first prove a stability condition for CSGLD based on the perturbation theory, and then verify regularity conditions for the solution of the Poisson equation so that the fluctuations of the mean-field system induced by CSGLD get controlled, which eventually ensures convergence of CSGLD.

Second, the use of the stochastic index  $J_{\tilde{U}}(\mathbf{x})$  in Eq.(8) avoids the evaluation of  $U(\mathbf{x})$  on the full data and thus significantly accelerates the computation of the algorithm, although it leads to a small bias, depending on the variance of the energy estimators, in parameter estimation. Compared to other methods, such as using a fixed sub-dataset to estimate  $U(\mathbf{x})$ , the implementation is much simpler. Moreover, combining the variance reduction of the noisy energy estimators [Deng et al., 2021], the bias also decreases to zero asymptotically as  $\epsilon \rightarrow 0$ .

Third, unlike the existing SGMCMC algorithms [Welling and Teh, 2011, Chen et al., 2014, Ma et al., 2015], CSGLD works as a *dynamic importance sampler* which *flattens* the target distribution and *reduces the energy barriers* for the sampler to traverse between different regions of the energy landscape (see Figure 1(a) for illustration). The sampling bias introduced thereby is accounted for by the importance weight  $\theta^\zeta(J_{\tilde{U}}(\cdot))$ . Interestingly, CSGLD possesses a *self-adjusting mechanism* to ease escapes from local traps, which is similar to the self-repulsive dynamics [Ye et al., 2020] and can be explained in Figure 2. That is, in order to escape from local traps, CSGLD is sometimes forced to **move toward higher energy regions by adopting negative learning rates**. This is a very attractive feature for simulations of multi-modal distributions.

### 3 Theoretical study of the CSGLD algorithm

In this section, we study the convergence of CSGLD algorithm under the framework of stochastic approximation and show the ergodicity property based on weighted averaging estimators.

#### 3.1 Convergence analysis

Following the tradition of stochastic approximation analysis, we rewrite the updating rule (10) as

$$\boldsymbol{\theta}_{k+1} = \boldsymbol{\theta}_k + \omega_{k+1} \tilde{H}(\boldsymbol{\theta}_k, \mathbf{x}_{k+1}), \quad (11)$$

where  $\tilde{H}(\boldsymbol{\theta}, \mathbf{x}) = (\tilde{H}_1(\boldsymbol{\theta}, \mathbf{x}), \dots, \tilde{H}_m(\boldsymbol{\theta}, \mathbf{x}))$  is a random field function with

$$\tilde{H}_i(\boldsymbol{\theta}, \mathbf{x}) = \theta^\zeta(J_{\tilde{U}}(\mathbf{x})) \left( 1_{i=J_{\tilde{U}}(\mathbf{x})} - \theta(i) \right), \quad i = 1, 2, \dots, m. \quad (12)$$

Notably,  $\tilde{H}(\boldsymbol{\theta}, \mathbf{x})$  works under an empirical measure  $\varpi_{\boldsymbol{\theta}}(\mathbf{x})$  which approximates the invariant measure  $\varpi_{\Psi_{\boldsymbol{\theta}}}(\mathbf{x}) \propto \frac{\pi(\mathbf{x})}{\Psi_{\boldsymbol{\theta}}^\zeta(U(\mathbf{x}))}$  asymptotically as  $\epsilon \rightarrow 0$  and  $n \rightarrow N$ . As shown in Lemma 1, we have

the mean-field equation

$$h(\boldsymbol{\theta}) = \int_{\mathcal{X}} \tilde{H}(\boldsymbol{\theta}, \mathbf{x}) \varpi_{\boldsymbol{\theta}}(\mathbf{x}) d\mathbf{x} = Z_{\boldsymbol{\theta}}^{-1} (\boldsymbol{\theta}_* + \varepsilon \beta(\boldsymbol{\theta}) - \boldsymbol{\theta}) = 0, \quad (13)$$

where  $\boldsymbol{\theta}_* = (\int_{\mathcal{X}_1} \pi(\mathbf{x}) d\mathbf{x}, \int_{\mathcal{X}_2} \pi(\mathbf{x}) d\mathbf{x}, \dots, \int_{\mathcal{X}_m} \pi(\mathbf{x}) d\mathbf{x})$ ,  $Z_{\boldsymbol{\theta}}$  is the normalizing constant,  $\beta(\boldsymbol{\theta})$  is a perturbation term,  $\varepsilon$  is a small error depending on  $\epsilon$ ,  $n$  and  $m$ . The mean-field equation implies that for any  $\zeta > 0$ ,  $\boldsymbol{\theta}_k$  converges to a small neighbourhood of  $\boldsymbol{\theta}_*$ . By applying perturbation theory and setting the Lyapunov function  $\mathbb{V}(\boldsymbol{\theta}) = \frac{1}{2} \|\boldsymbol{\theta}_* - \boldsymbol{\theta}\|^2$ , we can establish the stability condition:

**Lemma 1** (Stability, informal version of Lemma 3). *Given a small enough  $\epsilon$  (learning rate), a large enough  $n$  (batch size) and  $m$  (partition number), there is a constant  $\phi = \inf_{\boldsymbol{\theta}} Z_{\boldsymbol{\theta}}^{-1} > 0$  such that the mean-field  $h(\boldsymbol{\theta})$  satisfies*

$$\forall \boldsymbol{\theta} \in \Theta, \langle h(\boldsymbol{\theta}), \boldsymbol{\theta} - \boldsymbol{\theta}_* \rangle \leq -\phi \|\boldsymbol{\theta} - \boldsymbol{\theta}_*\|^2 + \mathcal{O} \left( \epsilon + \frac{1}{m} + \sup_{\mathbf{x}} \text{Var}(\xi_n(\mathbf{x})) \right),$$

where  $\text{Var}(\xi_n(\mathbf{x}))$  denotes the variance of the noise of the stochastic energy estimator  $\xi_n(\cdot)$  of batch size  $n$  and the variance decays to 0 as  $n \rightarrow N$ .

Together with the tool of Poisson equation [Benveniste et al., 1990, Andrieu et al., 2005], which controls the fluctuation of  $\tilde{H}(\boldsymbol{\theta}, \mathbf{x}) - h(\boldsymbol{\theta})$ , we can establish convergence of  $\boldsymbol{\theta}_k$  in Theorem 1, whose proof is given in the supplementary material.

**Theorem 1** ( $L^2$  convergence rate, informal version of Theorem 3). *Given standard smoothness and dissipativity assumptions, a small enough learning rate  $\epsilon_k$ , a large partition number  $m$  and a large batch size  $n$ ,  $\boldsymbol{\theta}_k$  converges to  $\boldsymbol{\theta}_*$  such that*

$$\mathbb{E} [\|\boldsymbol{\theta}_k - \boldsymbol{\theta}_*\|^2] = \mathcal{O} \left( \omega_k + \sup_{i \geq k_0} \epsilon_i + \frac{1}{m} + \sup_{\mathbf{x}} \text{Var}(\xi_n(\mathbf{x})) \right),$$

where  $k_0$  is some large enough integer and  $\boldsymbol{\theta}_* = (\int_{\mathcal{X}_1} \pi(\mathbf{x}) d\mathbf{x}, \int_{\mathcal{X}_2} \pi(\mathbf{x}) d\mathbf{x}, \dots, \int_{\mathcal{X}_m} \pi(\mathbf{x}) d\mathbf{x})$ .

### 3.2 Ergodicity and dynamic importance sampler

CSGLD belongs to the class of adaptive MCMC algorithms, but its transition kernel is based on SGLD instead of the Metropolis algorithm. As such, the ergodicity theory for traditional adaptive MCMC algorithms [Roberts and Rosenthal, 2007, Andrieu and Éric Moulines, 2006, Fort et al., 2011, Liang, 2010] is not directly applicable. To tackle this issue, we conduct the following theoretical study. First, rewrite (9) as

$$\mathbf{x}_k - \epsilon \left( \nabla_{\mathbf{x}} \hat{L}(\mathbf{x}_k, \boldsymbol{\theta}_*) + \Upsilon(\mathbf{x}_k, \boldsymbol{\theta}_k, \boldsymbol{\theta}_*) \right) + \mathcal{N}(0, 2\epsilon\tau \mathbf{I}), \quad (14)$$

where  $\nabla_{\mathbf{x}} \hat{L}(\mathbf{x}_k, \boldsymbol{\theta}_*) = \frac{N}{n} \left[ 1 + \frac{\zeta\tau}{\Delta u} (\log \theta_*(J(\mathbf{x}_k)) - \log \theta_*((J(\mathbf{x}_k) - 1) \vee 1)) \right] \nabla_{\mathbf{x}} \tilde{U}(\mathbf{x}_k)$ , the bias term  $\Upsilon(\mathbf{x}_k, \boldsymbol{\theta}_k, \boldsymbol{\theta}_*) = \nabla_{\mathbf{x}} \tilde{L}(\mathbf{x}_k, \boldsymbol{\theta}_k) - \nabla_{\mathbf{x}} \hat{L}(\mathbf{x}_k, \boldsymbol{\theta}_*)$ , and  $\nabla_{\mathbf{x}} \tilde{L}(\mathbf{x}_k, \boldsymbol{\theta}_k) = \frac{N}{n} \left[ 1 + \frac{\zeta\tau}{\Delta u} (\log \theta_k(J_{\tilde{V}}(\mathbf{x}_k)) - \log \theta_k((J_{\tilde{V}}(\mathbf{x}_k) - 1) \vee 1)) \right] \nabla_{\mathbf{x}} \tilde{U}(\mathbf{x}_k)$ . The order of the bias is figured out in Lemma C1 in the supplementary material based on the results of Theorem 1.

Next, we show how the empirical mean  $\frac{1}{k} \sum_{i=1}^k f(\mathbf{x}_i)$  deviates from the posterior mean  $\int_{\mathcal{X}} f(\mathbf{x}) \varpi_{\Psi_{\boldsymbol{\theta}_*}}(\mathbf{x}) d\mathbf{x}$ . Note that this is a direct application of Theorem 2 of Chen et al. [2015] by treating  $\nabla_{\mathbf{x}} \hat{L}(\mathbf{x}, \boldsymbol{\theta}_*)$  as the stochastic gradient of a target distribution and  $\Upsilon(\mathbf{x}, \boldsymbol{\theta}, \boldsymbol{\theta}_*)$  as the bias of the stochastic gradient. Moreover, considering that  $\varpi_{\tilde{\Psi}_{\boldsymbol{\theta}_*}}(\mathbf{x}) \propto \frac{\pi(\mathbf{x})}{\theta_*^{\zeta}(J(\mathbf{x}))} \rightarrow \varpi_{\Psi_{\boldsymbol{\theta}_*}}$  as  $m \rightarrow \infty$  based on Lemma B4 in the supplementary material, we have the following

**Lemma 2** (Convergence of the Averaging Estimators, informal version of Lemma 12). *Suppose the smoothness, dissipativity and other mild assumptions hold. For any bounded function  $f$ , we have*

$$\left| \mathbb{E} \left[ \frac{\sum_{i=1}^k f(\mathbf{x}_i)}{k} \right] - \int_{\mathcal{X}} f(\mathbf{x}) \varpi_{\tilde{\Psi}_{\boldsymbol{\theta}_*}}(d\mathbf{x}) \right| = \mathcal{O} \left( \frac{1}{k\epsilon} + \sqrt{\epsilon} + \sqrt{\frac{\sum_{i=1}^k \omega_k}{k}} + \frac{1}{\sqrt{m}} + \sup_{\mathbf{x}} \sqrt{\text{Var}(\xi_n(\mathbf{x}))} \right),$$

where  $\varpi_{\tilde{\Psi}_{\boldsymbol{\theta}_*}}(\mathbf{x}) = \frac{1}{Z_{\boldsymbol{\theta}_*} \theta_*^{\zeta}(J(\mathbf{x}))}$  and  $Z_{\boldsymbol{\theta}_*} = \sum_{i=1}^m \frac{\int_{\mathcal{X}_i} \pi(\mathbf{x}) d\mathbf{x}}{\theta_*(i)^{\zeta}}$ .

Finally, we consider the problem of estimating the quantity  $\int_{\mathcal{X}} f(\mathbf{x})\pi(\mathbf{x})d\mathbf{x}$ . Recall that  $\pi(\mathbf{x})$  is the target distribution that we would like to make inference for. To estimate this quantity, we naturally consider the weighted averaging estimator  $\frac{\sum_{i=1}^k \theta_i^\zeta(J_{\bar{U}}(\mathbf{x}_i))f(\mathbf{x}_i)}{\sum_{i=1}^k \theta_i^\zeta(J_{\bar{U}}(\mathbf{x}_i))}$  by treating  $\theta^\zeta(J_{\bar{U}}(\mathbf{x}_i))$  as the dynamic importance weight of the sample  $\mathbf{x}_i$  for  $i = 1, 2, \dots, k$ . The convergence of this estimator is established in Theorem 2, which can be proved by repeated applying Theorem 1 and Lemma 2 with the details given in the supplementary material.

**Theorem 2** (Convergence of the Weighted Averaging Estimators, informal version of Theorem 4). *Given the smoothness, dissipativity and other mild assumptions, for any bounded function  $f$ , we have*

$$\left| \mathbb{E} \left[ \frac{\sum_{i=1}^k \theta_i^\zeta(J_{\bar{U}}(\mathbf{x}_i))f(\mathbf{x}_i)}{\sum_{i=1}^k \theta_i^\zeta(J_{\bar{U}}(\mathbf{x}_i))} \right] - \int_{\mathcal{X}} f(\mathbf{x})\pi(d\mathbf{x}) \right| = \mathcal{O} \left( \frac{1}{k\epsilon} + \sqrt{\epsilon} + \sqrt{\frac{\sum_{i=1}^k \omega_k}{k}} + \frac{1}{\sqrt{m}} + \sup_{\mathbf{x}} \sqrt{\text{Var}(\xi_n(\mathbf{x}))} \right).$$

The bias of the weighted averaging estimator decreases if one applies a larger batch size, a finer sample space partition, a smaller learning rate  $\epsilon$ , and smaller step sizes  $\{\omega_k\}_{k \geq 0}$ . Admittedly, the order of this bias is slightly larger than  $\mathcal{O}(\frac{1}{k\epsilon} + \epsilon)$  achieved by the standard SGLD. We note that this is necessary as simulating from the flattened distribution  $\varpi_{\Psi_{\theta_*}}$  often leads to a much faster convergence, see e.g. the green curve v.s. the purple curve in Figure 1(c).

**Discussions on more scalable updates** The stochastic approximation update (7)(ii) yields a global stability property but may not be scalable enough in some big data problems. For more scalable updates, one can adopt an elegant stochastic approximation update proposed in Deng et al. [2022]

$$\theta_{k+1}(i) = \theta_k(i) + \omega_{k+1}\theta_k(J(\mathbf{x}_{k+1})) (1_{i=J(\mathbf{x}_{k+1})} - \theta_k(i)), \quad (15)$$

where  $\theta(i)$  converges to a smoother estimate of  $\left(\int_{\mathcal{X}_i} \pi(\mathbf{x})d\mathbf{x}\right)^{\frac{1}{\zeta}}$  instead of the original target  $\int_{\mathcal{X}_i} \pi(\mathbf{x})d\mathbf{x}$ . Since high energy region often yields exponentially decreasing probability mass, the exponent  $\frac{1}{\zeta}$  given  $\zeta \gg 1$  greatly facilitates the estimation tasks.

## 4 Numerical studies

### 4.1 Simulations of multi-modal distributions

**A Gaussian mixture distribution** The first numerical study is to test the performance of CSGLD on a Gaussian mixture distribution  $\pi(\mathbf{x}) = 0.4N(-6, 1) + 0.6N(4, 1)$ . In each experiment, the algorithm was run for  $10^7$  iterations. We fix the temperature  $\tau = 1$  and the learning rate  $\epsilon = 0.1$ . The step size for stochastic approximation follows  $\omega_k = \frac{1}{k^{0.6} + 100}$ . The sample space is partitioned into 50 subregions with  $\Delta u = 1$ . The stochastic gradients are simulated by injecting additional random noises following  $N(0, 0.01)$  to the exact gradients. For comparison, SGLD is chosen as the baseline algorithm and implemented with the same setup as CSGLD. We repeat the experiments 10 times and report the average and the associated standard deviation.

We first assume that  $\theta_*$  is known and plot the energy functions for both  $\pi(\mathbf{x})$  and  $\varpi_{\Psi_{\theta_*}}$  with different values of  $\zeta$ . Figure 1(a) shows that the original energy function has a rather large energy barrier which strongly affects the communication between two modes of the distribution. In contrast, CSGLD samples from a modified energy function, which yields a flattened landscape and reduced energy barriers. For example, with  $\zeta = 0.75$ , the energy barrier for this example is *greatly reduced from 12 to as small as 2*. Consequently, the local trap problem can be greatly alleviated. Regarding the bizarre peaks around  $x = 4$ , we leave the study in the supplementary material.

Figure 1(b) summarizes the estimates of  $\theta_*$  with  $\zeta = 0.75$ , which matches the ground truth value of  $\theta_*$  very well. Notably, we see that  $\theta_*(i)$  decays exponentially fast as the partition index  $i$  increases, which indicates the exponentially decreasing probability of visiting high energy regions and a severe local trap problem. CSGLD tackles this issue by adaptively updating the transition kernel or, equivalently, the invariant distribution such that the sampler moves like a “random walk” in the space of energy. In particular, setting  $\zeta = 1$  leads to a flat histogram of energy (for the samples produced by CSGLD).

To explore the performance of CSGLD in quantity estimation with the weighed averaging estimator, we compare CSGLD ( $\zeta = 0.75$ ) with SGLD and KSGLD in estimating the posterior mean

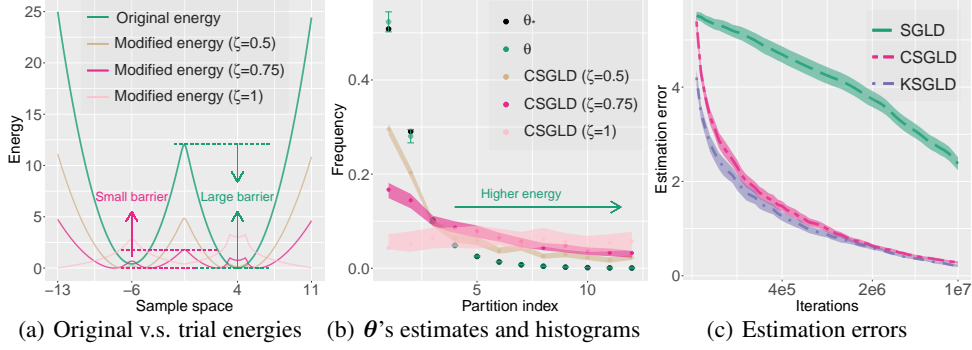


Figure 1: Comparison between SGLD and CSGLD: figure (a) presents only the first 12 partitions for an illustrative purpose; KSGLD in figure (c) is implemented by assuming  $\theta_*$  is known.

$\int_{\mathcal{X}} \mathbf{x} \pi(\mathbf{x}) d\mathbf{x}$ , where KSGLD was implemented by assuming  $\theta_*$  is known and sampling from  $\varpi_{\Psi_{\theta_*}}$  directly. Each algorithm was run for 10 times, and we recorded the mean absolute estimation error along with iterations. As shown in Figure 1(c), the estimation error of SGLD decays quite slow and rarely converges due to the high energy barrier. On the contrary, KSGLD converges much faster, which shows the advantage of sampling from a flattened distribution  $\varpi_{\Psi_{\theta_*}}$ . Admittedly,  $\theta_*$  is unknown in practice. CSGLD instead adaptively updates its invariant distribution while optimizing the parameter  $\theta$  until an *optimization-sampling equilibrium* is reached. In the early period of the run, CSGLD converges slightly slower than KSGLD, but soon it becomes as efficient as KSGLD.

Finally, we compare the sample path and learning rate for CSGLD and SGLD. As shown in Figure 2(a), SGLD tends to be trapped in a deep local optimum for an exponentially long time. CSGLD, in contrast, possesses a *self-adjusting mechanism* for escaping from local traps. In the early period of a run, CSGLD might suffer from a similar local-trap problem as SGLD (see Figure 2(b)). In this case, the components of  $\theta$  corresponding to the current subregion will increase very fast, eventually rendering a smaller or even negative gradient multiplier which *bounces the sampler back to high energy regions*. To illustrate the process, we plot a bouncy zone and an absorbing zone in Figure 2(c). The bouncy zone enables the sampler to “jump” over large energy barriers to explore other modes. As the run continues,  $\theta_k$  converges to  $\theta_*$ . Figure 2(d) shows that larger bouncy “jumps” (in red lines) can potentially be induced in the bouncy zone, which occurs in both local and global optima. Due to the *self-adjusting mechanism*, CSGLD has the local trap problem much alleviated.

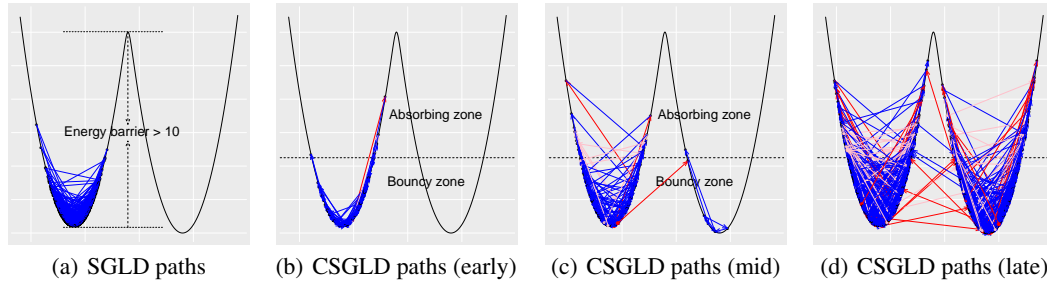


Figure 2: Sample trajectories of SGLD and CSGLD: figures (a) and (c) are implemented by 100,000 iterations with a thinning factor 100 and  $\zeta = 0.75$ , while figure (b) utilizes a thinning factor 10.

**A synthetic multi-modal distribution** We next simulate from a distribution  $\pi(\mathbf{x}) \propto e^{-U(\mathbf{x})}$ , where  $U(\mathbf{x}) = \sum_{i=1}^2 \frac{x(i)^2 - 10 \cos(1.2\pi x(i))}{3}$  and  $\mathbf{x} = (x(1), x(2))$ . We compare CSGLD with SGLD, replica exchange SGLD (reSGLD) [Deng et al., 2020], and SGLD with cyclic learning rates (cycSGLD) [Zhang et al., 2020] and detail the setups in the supplementary material. Figure 3(a) shows that the distribution contains nine important modes, where the center mode has the largest probability mass and the four modes on the corners have the smallest mass. We see in Figure 3(b) that SGLD spends too much time in local regions and only identifies three modes. cycSGLD has a better ability to explore the distribution by leveraging large learning rates cyclically. However, as illustrated in Figure 3(c), such a mechanism is still not efficient enough to resolve the local trap issue for this problem. reSGLD proposes to include a high-temperature process to encourage exploration and allows interactions between the two processes via appropriate swaps. We observe in Figure 3(d)

that reSGLD obtains both the exploration and exploitation abilities and yields a much better result. However, the noisy energy estimator may hinder the swapping efficiency and it becomes difficult to estimate a few modes on the corners. As to our algorithm, CSGLD first simulates the importance samples and recovers the original distribution according to the importance weights. We notice that the samples from CSGLD can traverse freely in the parameter space and eventually achieve a remarkable performance, as shown in Figure 3(e).

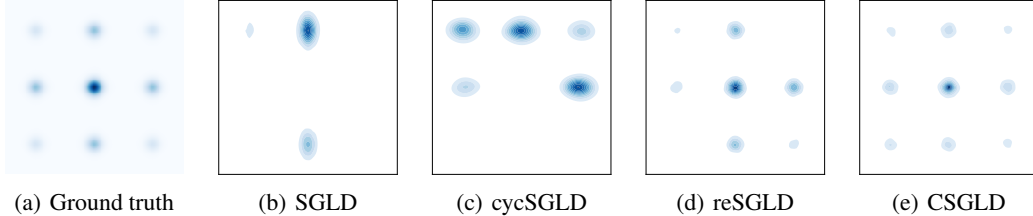


Figure 3: Simulations of a multi-modal distribution. A resampling scheme is used for CSGLD.

## 4.2 UCI data

We tested the performance of CSGLD on the **UCI** regression datasets. For each dataset, we normalized all features and randomly selected 10% of the observations for testing. Following [Hernandez-Lobato and Adams, 2015], we modeled the data using a Multi-Layer Perception (MLP) with a single hidden layer of 50 hidden units. We set the mini-batch size  $n = 50$  and trained the model for 5,000 epochs. The learning rate was set to  $5e-6$  and the default  $L_2$ -regularization coefficient is  $1e-4$ . For all the datasets, we used the stochastic energy  $\frac{N}{n}\tilde{U}(\mathbf{x})$  to evaluate the partition index. We set the energy bandwidth  $\Delta u = 100$ . We fine-tuned the temperature  $\tau$  and the hyperparameter  $\zeta$ . For a fair comparison, each algorithm was run 10 times with fixed seeds for each dataset. In each run, the performance of the algorithm was evaluated by averaging over 50 models, where the averaging estimator was used for SGD and SGLD and the weighted averaging estimator was used for CSGLD. As shown in Table 1, SGLD outperforms the stochastic gradient descent (SGD) algorithm for most datasets due to the advantage of a sampling algorithm in obtaining more informative modes. Since all these datasets are small, there is only very limited potential for improvement. Nevertheless, CSGLD still consistently outperforms all the baselines including SGD and SGLD.

The contour strategy proposed in the paper can be naturally extended to SGHMC [Chen et al., 2014, Ma et al., 2015] without affecting the theoretical results. In what follows, we adopted a numerical method proposed by Saatci and Wilson [2017] to avoid extra hyperparameter tuning. We set the momentum term to 0.9 and simply inherited all the other parameter settings used in the above experiments. In such a case, we compare the contour SGHMC (CSGHMC) with the baselines, including M-SGD (Momentum SGD) and SGHMC. The comparison indicates that some improvements can be achieved by including the momentum.

Table 1: Algorithm evaluation using average root-mean-square error and its standard deviation.

Dataset Hyperparameters ( $\tau/\zeta$ )	Energy 1/1	Concrete 5/1	Yacht 1/2.5	Wine 5/10
SGD	1.13±0.07	4.60±0.14	0.81±0.08	0.65±0.01
SGLD	1.08±0.07	4.12±0.10	0.72±0.07	0.63±0.01
CSGLD	<b>1.02±0.06</b>	<b>3.98±0.11</b>	<b>0.69±0.06</b>	<b>0.62±0.01</b>
M-SGD	0.95±0.07	4.32±0.27	0.73±0.08	0.71±0.02
SGHMC	0.77±0.06	4.25±0.19	<b>0.66±0.07</b>	0.67±0.02
CSGHMC	<b>0.76±0.06</b>	<b>4.15±0.20</b>	0.72±0.09	<b>0.65±0.01</b>

## 4.3 Computer vision data

This section compares only CSGHMC with M-SGD and SGHMC due to the popularity of momentum in accelerating computation for computer vision datasets. We keep partitioning the sample space according to the stochastic energy  $\frac{N}{n}\tilde{U}(\mathbf{x})$ , where a mini-batch data of size  $n$  is randomly chosen from the full dataset of size  $N$  at each iteration. Notably, such a strategy significantly accelerates the computation of CSGHMC. As a result, CSGHMC has almost the same computational cost as



SGHMC and SGD. To reduce the bias associated with the stochastic energy, we choose a large batch size  $n = 1,000$ . For more discussions on the hyperparameter settings, we refer readers to section D.4 in the supplementary material.

**CIFAR10** is a standard computer vision dataset with 10 classes and 60,000 images, for which 50,000 images were used for training and the rest for testing. We modeled the data using a Resnet of 20 layers (Resnet20) [He et al., 2016]. In particular, for CSGHMC, we considered a partition of the energy space in 200 subregions, where the energy bandwidth was set to  $\Delta u = 1000$ . We trained the model for a total of 1000 epochs and evaluated the model every ten epochs based on two criteria, namely, best point estimate (BPE) and Bayesian model average (BMA). We repeated each experiment 10 times and reported in Table 2 the average prediction accuracy and the standard deviation.

In the first set of experiments, all the algorithms utilized a fixed learning rate  $\epsilon = 2e - 7$  and a fixed temperature  $\tau = 0.01$  under the Bayesian setting. SGHMC performs quite similarly to M-SGD, both obtaining around 90% accuracy in BPE and 92% in BMA. Notably, in this case, simulated annealing is not applied to any of the algorithms and achieving the state-of-the-art is quite difficult. However, BMA still consistently outperforms BPE, implying the great potential of advanced MCMC techniques in deep learning. Instead of simulating from  $\pi(\mathbf{x})$  directly, CSGHMC adaptively simulates from a flattened distribution  $\varpi_{\theta_*}$  and adjusts the sampling bias by dynamic importance weights. As a result, the weighted averaging estimators obtain an improvement by as large as 0.8% on BMA. In addition, the flattened distribution facilitates optimization and the increase in BPE is quite significant.

In the second set of experiments, we employed a decaying schedule on both learning rates and temperatures (if applicable) to obtain simulated annealing effects. For the learning rate, we fix it at  $2 \times 10^{-6}$  in the first 400 epochs and then decayed it by a factor of 1.01 at each epoch. For the temperature, we consistently decayed it by a factor of 1.01 at each epoch. We call the resulting algorithms by saM-SGD, saSGHMC, and saCSGHMC, respectively. Table 2 shows that the performances of all algorithms are increased quite significantly, where the fine-tuned baselines already obtained the state-of-the-art results. Nevertheless, saCSGHMC further improves BPE by 0.25% and slightly improve the highly optimized BMA by nearly 0.1%.

**CIFAR100** dataset has 100 classes, each of which contains 500 training images and 100 testing images. We follow a similar setup as CIFAR10, except that  $\Delta u$  is set to 5000. For M-SGD, BMA can be better than BPE by as large as 5.6%. CSGHMC has led to an improvement of 3.5% on BPE and 2% on BMA, which further demonstrates the superiority of advanced MCMC techniques. Table 2 also shows that with the help of both simulated annealing and importance sampling, saCSGHMC can outperform the highly optimized baselines by almost 1% accuracy on BPE and 0.7% on BMA. The significant improvements show the advantage of the proposed method in training DNNs.

Table 2: Experiments on CIFAR10 & 100 using Resnet20, where BPE and BMA are short for best point estimate and Bayesian model average, respectively.

Algorithms	CIFAR10		CIFAR100	
	BPE	BMA	BPE	BMA
M-SGD	90.02±0.06	92.03±0.08	61.41±0.15	67.04±0.12
SGHMC	90.01±0.07	91.98±0.05	61.46±0.14	66.43±0.11
CSGHMC	<b>90.87±0.04</b>	<b>92.85±0.05</b>	<b>63.97±0.21</b>	<b>68.94±0.23</b>
saM-SGD	93.83±0.07	94.25±0.04	69.18±0.13	71.83±0.12
saSGHMC	93.80±0.06	94.24±0.06	69.24±0.11	71.98±0.10
saCSGHMC	<b>94.06±0.07</b>	94.33±0.07	<b>70.18±0.15</b>	<b>72.67±0.15</b>

## 5 Conclusion

We have proposed CSGLD as a general scalable Monte Carlo algorithm for both simulation and optimization tasks. CSGLD automatically adjusts the invariant distribution during simulations to facilitate escaping from local traps and traversing over the entire energy landscape. The sampling bias introduced thereby is accounted for by dynamic importance weights. We proved a stability condition for the mean-field system induced by CSGLD together with the convergence of its self-adapting parameter  $\theta$  to a unique fixed point  $\theta_*$ . We established the convergence of a weighted averaging estimator for CSGLD. The bias of the estimator decreases as we employ a finer partition, a larger mini-batch size, and smaller learning rates and step sizes. We tested CSGLD and its variants on a few examples, which show their great potential in deep learning and big data computing.

## Broader Impact

Our algorithm shows a potential to achieve free mode explorations in complex systems such as deep neural networks and greatly avoid the local trap problem. It is an extension of the flat histogram algorithms from the Metropolis kernel to the Langevin kernel and paves the way for future research in various dynamic importance samplers and adaptive biasing force (ABF) techniques for big data problems. The Bayesian community and the researchers in the area of Monte Carlo methods will enjoy the benefit of our work.

## Acknowledgment

Liang’s research was supported in part by the grants DMS-2015498, R01-GM117597 and R01-GM126089. Lin acknowledges the support from NSF (DMS-1555072, DMS-1736364), BNL Subcontract 382247, W911NF-15-1-0562, and DE-SC0021142.

## References

- Sungjin Ahn, Anoop Korattikara, and Max Welling. Bayesian Posterior Sampling via Stochastic Gradient Fisher Scoring. In *Proc. of the International Conference on Machine Learning (ICML)*, 2012.
- Christophe Andrieu and Éric Moulines. On the Ergodicity Properties of Some Adaptive MCMC Algorithms. *Annals of Applied Probability*, 16:1462–1505, 2006.
- Christophe Andrieu, Éric Moulines, and Pierre Priouret. Stability of Stochastic Approximation under Verifiable Conditions. *SIAM J. Control Optim.*, 44(1):283–312, 2005.
- Albert Benveniste, Michael Métivier, and Pierre Priouret. *Adaptive Algorithms and Stochastic Approximations*. Berlin: Springer, 1990.
- Bernd A. Berg and T. Neuhaus. Multicanonical Algorithms for First Order Phase Transitions. *Physics Letters B*, 267(2):249–253, 1991.
- Changyou Chen, Nan Ding, and Lawrence Carin. On the Convergence of Stochastic Gradient MCMC Algorithms with High-order Integrators. In *Advances in Neural Information Processing Systems (NeurIPS)*, pages 2278–2286, 2015.
- Tianqi Chen, Emily B. Fox, and Carlos Guestrin. Stochastic Gradient Hamiltonian Monte Carlo. In *Proc. of the International Conference on Machine Learning (ICML)*, 2014.
- Umut Şimşekli, Roland Badeau, A. Taylan Cemgil, and Gaë Richard. Stochastic Quasi-Newton Langevin Monte Carlo. In *Proc. of the International Conference on Machine Learning (ICML)*, pages 642–651, 2016.
- Wei Deng, Xiao Zhang, Faming Liang, and Guang Lin. An Adaptive Empirical Bayesian Method for Sparse Deep Learning. In *Advances in Neural Information Processing Systems (NeurIPS)*, 2019.
- Wei Deng, Qi Feng, Liyao Gao, Faming Liang, and Guang Lin. Non-Convex Learning via Replica Exchange Stochastic Gradient MCMC. In *Proc. of the International Conference on Machine Learning (ICML)*, 2020.
- Wei Deng, Qi Feng, Georgios Karagiannis, Guang Lin, and Faming Liang. Accelerating Convergence of Replica Exchange Stochastic Gradient MCMC via Variance Reduction. In *Proc. of the International Conference on Learning Representation (ICLR)*, 2021.
- Wei Deng, Siqi Liang, Botao Hao, Guang Lin, and Faming Liang. Interacting contour stochastic gradient langevin dynamics. In *Proc. of the International Conference on Learning Representation (ICLR)*, 2022.
- Nan Ding, Youhan Fang, Ryan Babbush, Changyou Chen, Robert D. Skeel, and Hartmut Neven. Bayesian Sampling using Stochastic Gradient Thermostats. In *Advances in Neural Information Processing Systems (NeurIPS)*, pages 3203–3211, 2014.

- Murat A Erdogdu, Lester Mackey, and Ohad Shamir. Global Non-convex Optimization with Discretized Diffusions. In *Advances in Neural Information Processing Systems (NeurIPS)*, 2018.
- G. Fort, É. Moulines, and P. Priouret. Convergence of Adaptive and Interacting Markov Chain Monte Carlo Algorithms. *Annals of Statistics*, 39:3262–3289, 2011.
- G. Fort, B. Jourdain, E. Kuhn, T. Lelièvre, and G. Stoltz. Convergence of the Wang-Landau Algorithm. *Math. Comput.*, 84(295):2297–2327, 2015.
- Charles J. Geyer. Markov Chain Monte Carlo Maximum Likelihood. *Computing Science and Statistics: Proceedings of the 23rd Symposium on the Interfac*, pages 156–163, 1991.
- W.K. Hastings. Monte Carlo Sampling Methods using Markov Chain and Their Applications. *Biometrika*, 57:97–109, 1970.
- Kaiming He, Xiangyu Zhang, Shaoqing Ren, and Jian Sun. Deep Residual Learning for Image Recognition. In *The IEEE Conference on Computer Vision and Pattern Recognition (CVPR)*, 2016.
- Jose Miguel Hernandez-Lobato and Ryan Adams. Probabilistic Backpropagation for Scalable Learning of Bayesian Neural Networks. In *Proc. of the International Conference on Machine Learning (ICML)*, volume 37, pages 1861–1869, 2015.
- Scott Kirkpatrick, D. Gelatt Jr, and Mario P. Vecchi. Optimization by Simulated Annealing. *Science*, 220(4598):671–680, 1983.
- T. Lelièvre, M. Rousset, and G. Stoltz. Long-time Convergence of an Adaptive Biasing Force Method. *Nonlinearity*, 21:1155–1181, 2008.
- Chunyu Li, Changyou Chen, David Carlson, and Lawrence Carin. Preconditioned Stochastic Gradient Langevin Dynamics for Deep Neural Networks. In *Proc. of the National Conference on Artificial Intelligence (AAAI)*, pages 1788–1794, 2016.
- Xuechen Li, Denny Wu, Lester Mackey, and Murat A. Erdogdu. Stochastic Runge-Kutta Accelerates Langevin Monte Carlo and Beyond. In *Advances in Neural Information Processing Systems (NeurIPS)*, pages 7746–7758, 2019.
- Faming Liang. A Generalized Wang–Landau Algorithm for Monte Carlo Computation. *Journal of the American Statistical Association*, 100(472):1311–1327, 2005.
- Faming Liang. On the Use of Stochastic Approximation Monte Carlo for Monte Carlo Integration. *Statistics and Probability Letters*, 79:581–587, 2009.
- Faming Liang. Trajectory Averaging for Stochastic Approximation MCMC Algorithms. *The Annals of Statistics*, 38:2823–2856, 2010.
- Faming Liang, Chuanhai Liu, and Raymond J. Carroll. Stochastic Approximation in Monte Carlo Computation. *Journal of the American Statistical Association*, 102:305–320, 2007.
- Yi-An Ma, Tianqi Chen, and Emily B. Fox. A Complete Recipe for Stochastic Gradient MCMC. In *Advances in Neural Information Processing Systems (NeurIPS)*, 2015.
- Oren Mangoubi and Nisheeth K. Vishnoi. Convex Optimization with Unbounded Nonconvex Oracles using Simulated Annealing. In *Proc. of Conference on Learning Theory (COLT)*, 2018.
- J.C. Mattingly, A.M. Stuart, and D.J. Higham. Ergodicity for SDEs and Approximations: Locally Lipschitz Vector Fields and Degenerate Noise. *Stochastic Processes and their Applications*, 101: 185–232, 2002.
- Jonathan C. Mattingly, Andrew M. Stuart, and M.V. Tretyakov. Convergence of Numerical Time-Averaging and Stationary Measures via Poisson Equations. *SIAM Journal on Numerical Analysis*, 48:552–577, 2010.
- N. Metropolis, A.W. Rosenbluth, M.N. Rosenbluth, A.H. Teller, and E. Teller. Equation of State Calculations by Fast Computing Machines. *Journal of Chemical Physics*, 21:1087–1091, 1953.

- Adam Paszke, Sam Gross, Soumith Chintala, Gregory Chanan, Edward Yang, Zachary DeVito, Zeming Lin, Alban Desmaison, Luca Antiga, and Adam Lerer. Automatic differentiation in PyTorch. In *NeurIPS Autodiff Workshop*, 2017.
- Maxim Raginsky, Alexander Rakhlin, and Matus Telgarsky. Non-convex Learning via Stochastic Gradient Langevin Dynamics: a Nonasymptotic Analysis. In *Proc. of Conference on Learning Theory (COLT)*, June 2017.
- Herbert Robbins and Sutton Monro. A Stochastic Approximation Method. *Annals of Mathematical Statistics*, 22:400–407, 1951.
- Gerneth O. Roberts and Jeff S. Rosenthal. Coupling and Ergodicity of Adaptive Markov Chain Monte Carlo Algorithms. *Journal of Applied Probability*, 44:458–475, 2007.
- Yunus Saatci and Andrew G Wilson. Bayesian GAN. In *Advances in Neural Information Processing Systems (NeurIPS)*, pages 3622–3631, 2017.
- Issei Sato and Hiroshi Nakagawa. Approximation Analysis of Stochastic Gradient Langevin Dynamics by Using Fokker-Planck Equation and Ito Process. In *Proc. of the International Conference on Machine Learning (ICML)*, 2014.
- Robert H. Swendsen and Jian-Sheng Wang. Replica Monte Carlo Simulation of Spin-Glasses. *Physical Review Letters*, 57:2607–2609, 1986.
- Yee Whye Teh, Alexandre Thiery, and Sebastian Vollmer. Consistency and Fluctuations for Stochastic Gradient Langevin Dynamics. *Journal of Machine Learning Research*, 17:1–33, 2016.
- Eric Vanden-Eijnden. Introduction to Regular Perturbation Theory. *Slides*, 2001. URL [https://cims.nyu.edu/~eve2/reg\\_pert.pdf](https://cims.nyu.edu/~eve2/reg_pert.pdf).
- Sebastian J. Vollmer, Konstantinos C. Zygalakis, and Yee Whye Teh. Exploration of the (Non-) Asymptotic Bias and Variance of Stochastic Gradient Langevin Dynamics. *Journal of Machine Learning Research*, 17(159):1–48, 2016.
- Fugao Wang and D. P. Landau. Efficient, Multiple-range Random Walk Algorithm to Calculate the Density of States. *Physical Review Letters*, 86(10):2050–2053, 2001.
- Max Welling and Yee Whye Teh. Bayesian Learning via Stochastic Gradient Langevin Dynamics. In *Proc. of the International Conference on Machine Learning (ICML)*, pages 681–688, 2011.
- Pan Xu, Jinghui Chen, Difan Zou, and Quanquan Gu. Global Convergence of Langevin Dynamics Based Algorithms for Nonconvex Optimization. In *Advances in Neural Information Processing Systems (NeurIPS)*, 2018.
- Mao Ye, Tongzheng Ren, and Qiang Liu. Stein Self-Repulsive Dynamics: Benefits From Past Samples. *arXiv:2002.09070v1*, 2020.
- Ruqi Zhang, Chunyuan Li, Jianyi Zhang, Changyou Chen, and Andrew Gordon Wilson. Cyclical Stochastic Gradient MCMC for Bayesian Deep Learning. In *Proc. of the International Conference on Learning Representation (ICLR)*, 2020.
- Yuchen Zhang, Percy Liang, and Moses Charikar. A Hitting Time Analysis of Stochastic Gradient Langevin Dynamics. In *Proc. of Conference on Learning Theory (COLT)*, pages 1980–2022, 2017.

## Supplementary Material for “A Contour Stochastic Gradient Langevin Dynamics Algorithm for Simulations of Multi-modal Distributions”

The supplementary material is organized as follows: Section **A** provides a review for the related methodologies, Section **B** proves the stability condition and convergence of the self-adapting parameter, Section **C** establishes the ergodicity of the contour stochastic gradient Langevin dynamics (CSGLD) algorithm, and Section **D** provides more discussions for the algorithm.

### A Background on stochastic approximation and Poisson equation

#### A.1 Stochastic approximation

Stochastic approximation [Benveniste et al., 1990] provides a standard framework for the development of adaptive algorithms. Given a random field function  $\tilde{H}(\boldsymbol{\theta}, \boldsymbol{x})$ , the goal of the stochastic approximation algorithm is to find the solution to the mean-field equation  $h(\boldsymbol{\theta}) = 0$ , i.e., solving

$$h(\boldsymbol{\theta}) = \int_{\mathcal{X}} \tilde{H}(\boldsymbol{\theta}, \boldsymbol{x}) \varpi_{\boldsymbol{\theta}}(d\boldsymbol{x}) = 0,$$

where  $\boldsymbol{x} \in \mathcal{X} \subset \mathbb{R}^d$ ,  $\boldsymbol{\theta} \in \Theta \subset \mathbb{R}^m$ ,  $\tilde{H}(\boldsymbol{\theta}, \boldsymbol{x})$  is a random field function and  $\varpi_{\boldsymbol{\theta}}(\boldsymbol{x})$  is a distribution function of  $\boldsymbol{x}$  depending on the parameter  $\boldsymbol{\theta}$ . The stochastic approximation algorithm works by repeating the following iterations

- (1) Draw  $\boldsymbol{x}_{k+1} \sim \Pi_{\boldsymbol{\theta}_k}(\boldsymbol{x}_k, \cdot)$ , where  $\Pi_{\boldsymbol{\theta}_k}(\boldsymbol{x}_k, \cdot)$  is a transition kernel that admits  $\varpi_{\boldsymbol{\theta}_k}(\boldsymbol{x})$  as the invariant distribution,
- (2) Update  $\boldsymbol{\theta}_{k+1} = \boldsymbol{\theta}_k + \omega_{k+1} \tilde{H}(\boldsymbol{\theta}_k, \boldsymbol{x}_{k+1}) + \omega_{k+1}^2 \rho(\boldsymbol{\theta}_k, \boldsymbol{x}_{k+1})$ , where  $\rho(\cdot, \cdot)$  denotes a bias term.

The algorithm differs from the Robbins–Monro algorithm [Robbins and Monro, 1951] in that  $\boldsymbol{x}$  is simulated from a transition kernel  $\Pi_{\boldsymbol{\theta}_k}(\cdot, \cdot)$  instead of the exact distribution  $\varpi_{\boldsymbol{\theta}_k}(\cdot)$ . As a result, a Markov state-dependent noise  $\tilde{H}(\boldsymbol{\theta}_k, \boldsymbol{x}_{k+1}) - h(\boldsymbol{\theta}_k)$  is generated, which requires some regularity conditions to control the fluctuation  $\sum_k \Pi_{\boldsymbol{\theta}}^k(\tilde{H}(\boldsymbol{\theta}, \boldsymbol{x}) - h(\boldsymbol{\theta}))$ . Moreover, it supports a more general form where a bounded bias term  $\rho(\cdot, \cdot)$  is allowed without affecting the theoretical properties of the algorithm.

#### A.2 Poisson equation

Stochastic approximation generates a nonhomogeneous Markov chain  $\{(\boldsymbol{x}_k, \boldsymbol{\theta}_k)\}_{k=1}^{\infty}$ , for which the convergence theory can be studied based on the Poisson equation

$$\mu_{\boldsymbol{\theta}}(\boldsymbol{x}) - \Pi_{\boldsymbol{\theta}} \mu_{\boldsymbol{\theta}}(\boldsymbol{x}) = \tilde{H}(\boldsymbol{\theta}, \boldsymbol{x}) - h(\boldsymbol{\theta}),$$

where  $\Pi_{\boldsymbol{\theta}}(\boldsymbol{x}, A)$  is the transition kernel for any Borel subset  $A \subset \mathcal{X}$  and  $\mu_{\boldsymbol{\theta}}(\cdot)$  is a function on  $\mathcal{X}$ . The solution to the Poisson equation exists when the following series converges:

$$\mu_{\boldsymbol{\theta}}(\boldsymbol{x}) := \sum_{k \geq 0} \Pi_{\boldsymbol{\theta}}^k(\tilde{H}(\boldsymbol{\theta}, \boldsymbol{x}) - h(\boldsymbol{\theta})).$$

That is, the consistency of the estimator  $\boldsymbol{\theta}$  can be established by controlling the perturbations of  $\sum_{k \geq 0} \Pi_{\boldsymbol{\theta}}^k(\tilde{H}(\boldsymbol{\theta}, \boldsymbol{x}) - h(\boldsymbol{\theta}))$  via imposing some regularity conditions on  $\mu_{\boldsymbol{\theta}}(\cdot)$ . Towards this goal, Benveniste et al. [1990] gave the following regularity conditions on  $\mu_{\boldsymbol{\theta}}(\cdot)$  to ensure the convergence of the adaptive algorithm:

There exist a function  $V : \mathcal{X} \rightarrow [1, \infty)$ , and a constant  $C$  such that for all  $\boldsymbol{\theta}, \boldsymbol{\theta}' \in \Theta$ ,

$$\|\Pi_{\boldsymbol{\theta}} \mu_{\boldsymbol{\theta}}(\boldsymbol{x})\| \leq CV(\boldsymbol{x}), \quad \|\Pi_{\boldsymbol{\theta}} \mu_{\boldsymbol{\theta}}(\boldsymbol{x}) - \Pi_{\boldsymbol{\theta}'} \mu_{\boldsymbol{\theta}'}(\boldsymbol{x})\| \leq C \|\boldsymbol{\theta} - \boldsymbol{\theta}'\| V(\boldsymbol{x}), \quad \mathbb{E}[V(\boldsymbol{x})] \leq \infty,$$

which requires only the first order smoothness. In contrast, the ergodicity theory by Mattingly et al. [2010] and Vollmer et al. [2016] relies on the much stronger 4th order smoothness.

## B Stability and convergence analysis for CSGLD

### B.1 CSGLD algorithm

To make the theory more general, we slightly extend CSGLD by allowing a higher order bias term. The resulting algorithm works by iterating between the following two steps:

$$(1) \text{ Sample } \mathbf{x}_{k+1} = \mathbf{x}_k - \epsilon_k \nabla_{\mathbf{x}} \tilde{L}(\mathbf{x}_k, \boldsymbol{\theta}_k) + \mathcal{N}(0, 2\epsilon_k \tau \mathbf{I}), \quad (\text{S}_1)$$

$$(2) \text{ Update } \boldsymbol{\theta}_{k+1} = \boldsymbol{\theta}_k + \omega_{k+1} \tilde{H}(\boldsymbol{\theta}_k, \mathbf{x}_{k+1}) + \omega_{k+1}^2 \rho(\boldsymbol{\theta}_k, \mathbf{x}_{k+1}), \quad (\text{S}_2)$$

where  $\epsilon_k$  is the learning rate,  $\omega_{k+1}$  is the step size,  $\nabla_{\mathbf{x}} \tilde{L}(\mathbf{x}, \boldsymbol{\theta})$  is the stochastic gradient given by

$$\nabla_{\mathbf{x}} \tilde{L}(\mathbf{x}, \boldsymbol{\theta}) = \frac{N}{n} \left[ 1 + \frac{\zeta \tau}{\Delta u} (\log \theta(J_{\tilde{U}}(\mathbf{x})) - \log \theta((J_{\tilde{U}}(\mathbf{x}) - 1) \vee 1)) \right] \nabla_{\mathbf{x}} \tilde{U}(\mathbf{x}), \quad (16)$$

$\tilde{H}(\boldsymbol{\theta}, \mathbf{x}) = (\tilde{H}_1(\boldsymbol{\theta}, \mathbf{x}), \dots, \tilde{H}_m(\boldsymbol{\theta}, \mathbf{x}))$  is a random field function with

$$\tilde{H}_i(\boldsymbol{\theta}, \mathbf{x}) = \theta^\zeta(J_{\tilde{U}}(\mathbf{x})) \left( 1_{i=J_{\tilde{U}}(\mathbf{x})} - \theta(i) \right), \quad i = 1, 2, \dots, m, \quad (17)$$

for some constant  $\zeta > 0$ , and  $\rho(\boldsymbol{\theta}_k, \mathbf{x}_{k+1})$  is a bias term.

### B.2 Convergence of parameter estimation

To establish the convergence of  $\boldsymbol{\theta}_k$ , we make the following assumptions:

**Assumption A1** (Compactness). *The space  $\Theta$  is compact such that  $\inf_{\Theta} \theta(i) > 0$  for any  $i \in \{1, 2, \dots, m\}$ ; the perturbation term  $\rho(\boldsymbol{\theta}, \mathbf{x})$  is also uniformly bounded for any  $\mathbf{x} \in \mathcal{X}$  and  $\boldsymbol{\theta} \in \Theta$ .*

To simplify the proof, we consider a slightly stronger assumption such that  $\inf_{\Theta} \theta(i) > 0$  holds for any  $i \in \{1, 2, \dots, m\}$ . To relax this assumption, we refer interested readers to [Fort et al. \[2015\]](#) where the recurrence property was proved for the sequence  $\{\boldsymbol{\theta}_k\}_{k \geq 1}$  of a similar algorithm. Such a property guarantees  $\boldsymbol{\theta}_k$  to visit often enough to a desired compact space, rendering the convergence of the sequence.

By Assumption A1 and Eq.(17), it is easy to conclude that there exists a constant  $Q > 0$  such that for any  $\boldsymbol{\theta} \in \Theta$  and  $\mathbf{x} \in \mathcal{X}$ ,

$$\|\boldsymbol{\theta}\| \leq Q, \quad \|\tilde{H}(\boldsymbol{\theta}, \mathbf{x})\| \leq Q, \quad \|\rho(\boldsymbol{\theta}, \mathbf{x})\| \leq Q. \quad (18)$$

**Assumption A2** (Smoothness).  *$U(\mathbf{x})$  is  $M$ -smooth; that is, there exists a constant  $M > 0$  such that for any  $\mathbf{x}, \mathbf{x}' \in \mathcal{X}$ ,*

$$\|\nabla_{\mathbf{x}} U(\mathbf{x}) - \nabla_{\mathbf{x}} U(\mathbf{x}')\| \leq M \|\mathbf{x} - \mathbf{x}'\|. \quad (19)$$

Smoothness is a standard assumption in the study of convergence of SGLD, see e.g. [Raginsky et al. \[2017\]](#), [Xu et al. \[2018\]](#).

**Assumption A3** (Dissipativity). *There exist constants  $\tilde{m} > 0$  and  $\tilde{b} \geq 0$  such that for any  $\mathbf{x} \in \mathcal{X}$  and  $\boldsymbol{\theta} \in \Theta$ ,*

$$\langle \nabla_{\mathbf{x}} L(\mathbf{x}, \boldsymbol{\theta}), \mathbf{x} \rangle \leq \tilde{b} - \tilde{m} \|\mathbf{x}\|^2. \quad (20)$$

This assumption ensures samples to move towards the origin regardless the initial point, which is standard in proving the geometric ergodicity of dynamical systems, see e.g. [Mattingly et al. \[2002\]](#), [Raginsky et al. \[2017\]](#), [Xu et al. \[2018\]](#).

**Assumption A4** (Gradient noise). *The stochastic gradient is unbiased, that is,*

$$\mathbb{E}[\nabla_{\mathbf{x}} \tilde{U}(\mathbf{x}_k) - \nabla_{\mathbf{x}} U(\mathbf{x}_k)] = 0;$$

*in addition, there exist some constants  $M > 0$  and  $B > 0$  such that*

$$\mathbb{E}[\|\nabla_{\mathbf{x}} \tilde{U}(\mathbf{x}_k) - \nabla_{\mathbf{x}} U(\mathbf{x}_k)\|^2] \leq M^2 \|\mathbf{x}\|^2 + B^2,$$

*where the expectation  $\mathbb{E}[\cdot]$  is taken with respect to the distribution of the noise component in  $\nabla_{\mathbf{x}} \tilde{U}(\mathbf{x})$ .*

Lemma 3 establishes a stability condition for CSGLD, which implies potential convergence of  $\theta_k$ .

**Lemma 3** (Stability, restatement of Lemma 1). *Suppose that Assumptions A1-A4 hold. For any  $\theta \in \Theta$ ,  $\langle h(\theta), \theta - \theta_* \rangle \leq -\phi \|\theta - \theta_*\|^2 + \mathcal{O}(\sup_{\mathbf{x}} \text{Var}(\xi_n(\mathbf{x})) + \epsilon + \frac{1}{m})$ , where  $\phi = \inf_{\theta} Z_{\theta}^{-1} > 0$ ,  $\theta_* = (\int_{\mathcal{X}_1} \pi(\mathbf{x}) d\mathbf{x}, \int_{\mathcal{X}_2} \pi(\mathbf{x}) d\mathbf{x}, \dots, \int_{\mathcal{X}_m} \pi(\mathbf{x}) d\mathbf{x})$ ,  $\text{Var}(\xi_n(\cdot))$  denotes the variance of the noise of the stochastic energy estimator  $\xi_n(\cdot)$  of batch size  $n$  and it decays to 0 as  $n \rightarrow N$ .*

**Proof** Let  $\varpi_{\Psi_{\theta}}(\mathbf{x}) \propto \frac{\pi(\mathbf{x})}{\Psi_{\theta}^{\zeta}(U(\mathbf{x}))}$  denote a theoretical invariant measure of SGLD, where  $\Psi_{\theta}(u)$  is a fixed piecewise continuous function given by

$$\Psi_{\theta}(u) = \sum_{i=1}^m \left( \theta(i-1) e^{(\log \theta(i) - \log \theta(i-1)) \frac{u - u_{i-1}}{\Delta u}} \right) 1_{u_{i-1} < u \leq u_i}, \quad (21)$$

the full data is used in determining the indexes of subregions, and the learning rate converges to zero. In addition, we define a piece-wise constant function

$$\tilde{\Psi}_{\theta} = \sum_{i=1}^m \theta(i) 1_{u_{i-1} < u \leq u_i},$$

and a theoretical measure  $\varpi_{\tilde{\Psi}_{\theta}}(\mathbf{x}) \propto \frac{\pi(\mathbf{x})}{\theta^{\zeta}(J(\mathbf{x}))}$ . Obviously, as the sample space partition becomes fine and fine, i.e.,  $u_1 \rightarrow u_{\min}$ ,  $u_{m-1} \rightarrow u_{\max}$  and  $m \rightarrow \infty$ , we have  $\|\tilde{\Psi}_{\theta} - \Psi_{\theta}\| \rightarrow 0$  and  $\|\varpi_{\tilde{\Psi}_{\theta}}(\mathbf{x}) - \varpi_{\Psi_{\theta}}(\mathbf{x})\| \rightarrow 0$ , where  $u_{\min}$  and  $u_{\max}$  denote the minimum and maximum of  $U(\mathbf{x})$ , respectively. Without loss of generality, we assume  $u_{\max} < \infty$ . Otherwise,  $u_{\max}$  can be set to a value such that  $\pi(\{\mathbf{x} : U(\mathbf{x}) > u_{\max}\})$  is sufficiently small.

For each  $i \in \{1, 2, \dots, m\}$ , the random field  $\tilde{H}_i(\theta, \mathbf{x}) = \theta^{\zeta}(J_{\tilde{v}}(\mathbf{x})) (1_{i \geq J_{\tilde{v}}(\mathbf{x})} - \theta(i))$  is a biased estimator of  $H_i(\theta, \mathbf{x}) = \theta^{\zeta}(J(\mathbf{x})) (1_{i \geq J(\mathbf{x})} - \theta(i))$ . By Lemma 4 of [Deng et al., 2022], the bias caused by the mini-batch energy estimator follows  $\mathbb{E}[\tilde{H}(\theta, \mathbf{x}) - H(\theta, \mathbf{x})] = \mathcal{O}(\sup_{\mathbf{x}} \text{Var}(\xi_n(\mathbf{x})))$ , where  $\xi_n(\cdot)$  is the noisy energy estimator of batch size  $n$  and  $\text{Var}(\cdot)$  denotes the variance.

First, let's compute the mean-field  $h(\theta)$  with respect to the empirical measure  $\varpi_{\theta}(\mathbf{x})$ :

$$\begin{aligned} h_i(\theta) &= \int_{\mathcal{X}} \tilde{H}_i(\theta, \mathbf{x}) \varpi_{\theta}(\mathbf{x}) d\mathbf{x} = \int_{\mathcal{X}} H_i(\theta, \mathbf{x}) \varpi_{\theta}(\mathbf{x}) d\mathbf{x} + \mathcal{O}\left(\sup_{\mathbf{x}} \text{Var}(\xi_n(\mathbf{x}))\right) \\ &= \int_{\mathcal{X}} H_i(\theta, \mathbf{x}) \left( \underbrace{\varpi_{\tilde{\Psi}_{\theta}}(\mathbf{x})}_{I_1} - \underbrace{\varpi_{\tilde{\Psi}_{\theta}}(\mathbf{x}) + \varpi_{\Psi_{\theta}}(\mathbf{x}) - \varpi_{\Psi_{\theta}}(\mathbf{x})}_{I_2: \text{piece-wise approximation}} + \underbrace{\varpi_{\theta}(\mathbf{x})}_{I_3: \text{discretization}} \right) d\mathbf{x} + \mathcal{O}\left(\sup_{\mathbf{x}} \text{Var}(\xi_n(\mathbf{x}))\right). \end{aligned} \quad (22)$$

(i) For the term  $I_1$ , we have

$$\begin{aligned} \int_{\mathcal{X}} H_i(\theta, \mathbf{x}) \varpi_{\tilde{\Psi}_{\theta}}(\mathbf{x}) d\mathbf{x} &= \frac{1}{Z_{\theta}} \int_{\mathcal{X}} \theta^{\zeta}(J(\mathbf{x})) (1_{i \geq J(\mathbf{x})} - \theta(i)) \frac{\pi(\mathbf{x})}{\theta^{\zeta}(J(\mathbf{x}))} d\mathbf{x} \\ &= Z_{\theta}^{-1} \left[ \sum_{k=1}^m \int_{\mathcal{X}_k} \pi(\mathbf{x}) 1_{k=i} d\mathbf{x} - \theta(i) \sum_{k=1}^m \int_{\mathcal{X}_k} \pi(\mathbf{x}) d\mathbf{x} \right] \\ &= Z_{\theta}^{-1} [\theta_*(i) - \theta(i)], \end{aligned} \quad (23)$$

where  $Z_{\theta} = \sum_{i=1}^m \frac{\int_{\mathcal{X}_i} \pi(\mathbf{x}) d\mathbf{x}}{\theta(i)^{\zeta}}$  denotes the normalizing constant of  $\varpi_{\tilde{\Psi}_{\theta}}(\mathbf{x})$ .

(ii) As to the integral  $I_2$ . By Lemma 6 and the boundedness of  $H(\theta, \mathbf{x})$ , we have

$$\int_{\mathcal{X}} H_i(\theta, \mathbf{x}) (-\varpi_{\tilde{\Psi}_{\theta}}(\mathbf{x}) + \varpi_{\Psi_{\theta}}(\mathbf{x})) d\mathbf{x} = \mathcal{O}\left(\frac{1}{m}\right). \quad (24)$$

(iii) Regarding the term  $I_3$ , we have for any fixed  $\theta$ ,

$$\int_{\mathcal{X}} H_i(\theta, \mathbf{x}) (-\varpi_{\Psi_{\theta}}(\mathbf{x}) + \varpi_{\theta}(\mathbf{x})) d\mathbf{x} = \mathcal{O}(\epsilon), \quad (25)$$

where the order of  $\mathcal{O}(\epsilon)$  follows from Theorem 6 of [Sato and Nakagawa \[2014\]](#).

Plugging (23), (24) and (25) into (22), we have

$$h_i(\boldsymbol{\theta}) = Z_{\boldsymbol{\theta}}^{-1} [\varepsilon\beta_i(\boldsymbol{\theta}) + \boldsymbol{\theta}_*(i) - \theta(i)], \quad (26)$$

where  $\varepsilon = \mathcal{O}(\sup_{\mathbf{x}} \text{Var}(\xi_n(\mathbf{x})) + \epsilon + \frac{1}{m})$  and  $\beta_i(\boldsymbol{\theta})$  is a bounded term such that  $Z_{\boldsymbol{\theta}}^{-1}\varepsilon\beta_i(\boldsymbol{\theta}) = \mathcal{O}(\sup_{\mathbf{x}} \text{Var}(\xi_n(\mathbf{x})) + \epsilon + \frac{1}{m})$ .

To solve the ODE system with small disturbances, we consider standard techniques in perturbation theory. According to the fundamental theorem of perturbation theory [[Vanden-Eijnden, 2001](#)], we can obtain the solution to the mean field equation  $h(\boldsymbol{\theta}) = 0$ :

$$\theta(i) = \boldsymbol{\theta}_*(i) + \varepsilon\beta_i(\boldsymbol{\theta}_*) + \mathcal{O}(\varepsilon^2), \quad i = 1, 2, \dots, m, \quad (27)$$

which is a stable point in a small neighbourhood of  $\boldsymbol{\theta}_*$ .

Considering the positive definite function  $\mathbb{V}(\boldsymbol{\theta}) = \frac{1}{2}\|\boldsymbol{\theta}_* - \boldsymbol{\theta}\|^2$  for the mean-field system  $h(\boldsymbol{\theta}) = Z_{\boldsymbol{\theta}}^{-1}(\varepsilon\beta_i(\boldsymbol{\theta}) + \boldsymbol{\theta}_* - \boldsymbol{\theta}) = Z_{\boldsymbol{\theta}}^{-1}(\boldsymbol{\theta}_* - \boldsymbol{\theta}) + \mathcal{O}(\varepsilon)$ , we have

$$\begin{aligned} \langle h(\boldsymbol{\theta}), \mathbb{V}(\boldsymbol{\theta}) \rangle &= \langle h(\boldsymbol{\theta}), \boldsymbol{\theta} - \boldsymbol{\theta}_* \rangle \\ &= -Z_{\boldsymbol{\theta}}^{-1}\|\boldsymbol{\theta} - \boldsymbol{\theta}_*\|^2 + \mathcal{O}(\varepsilon) \\ &\leq -\phi\|\boldsymbol{\theta} - \boldsymbol{\theta}_*\|^2 + \mathcal{O}\left(\sup_{\mathbf{x}} \text{Var}(\xi_n(\mathbf{x})) + \epsilon + \frac{1}{m}\right), \end{aligned}$$

where  $\phi = \inf_{\boldsymbol{\theta}} Z_{\boldsymbol{\theta}}^{-1} > 0$  by the compactness assumption [A1](#). This concludes the proof.

The following is a restatement of Lemma 3.2 [[Raginsky et al., 2017](#)], which holds for any  $\boldsymbol{\theta}$  in the compact space  $\Theta$ . Similar results have been shown in [Deng et al. \[2019\]](#).

**Lemma 4** (Uniform  $L^2$  bounds). *Suppose Assumptions [A1](#), [A3](#) and [A4](#) hold. Given a small enough learning rate, then  $\sup_{k \geq 1} \mathbb{E}[\|\mathbf{x}_k\|^2] < \infty$ .*

To ensure the perturbations of the stochastic approximation process decays sufficiently fast, we present the following result on the regularity properties.

**Lemma 5** (Solution of Poisson equation). *Suppose that Assumptions [A1](#)-[A4](#) hold. There is a solution  $\mu_{\boldsymbol{\theta}}(\cdot)$  on  $\mathcal{X}$  to the Poisson equation*

$$\mu_{\boldsymbol{\theta}}(\mathbf{x}) - \Pi_{\boldsymbol{\theta}}\mu_{\boldsymbol{\theta}}(\mathbf{x}) = \tilde{H}(\boldsymbol{\theta}, \mathbf{x}) - h(\boldsymbol{\theta}). \quad (28)$$

In addition, for all  $\boldsymbol{\theta}, \boldsymbol{\theta}' \in \Theta$ , there exists a constant  $C$  such that

$$\begin{aligned} \mathbb{E}[\|\Pi_{\boldsymbol{\theta}}\mu_{\boldsymbol{\theta}}(\mathbf{x})\|] &\leq C, \\ \mathbb{E}[\|\Pi_{\boldsymbol{\theta}}\mu_{\boldsymbol{\theta}}(\mathbf{x}) - \Pi_{\boldsymbol{\theta}'}\mu_{\boldsymbol{\theta}'}(\mathbf{x})\|] &\leq C\|\boldsymbol{\theta} - \boldsymbol{\theta}'\|. \end{aligned} \quad (29)$$

**Proof** The proof hinges on verifying drift conditions proposed in Section 6 of [[Andrieu et al., 2005](#)] and the details have been given in Lemma 6 of [Deng et al. \[2022\]](#).

Now we are ready to prove the first main result on the convergence of  $\boldsymbol{\theta}_k$ . The technique lemmas are listed in Section [B.3](#).

**Assumption A5** (Learning rate and step size). *The learning rate  $\{\epsilon_k\}_{k \in \mathbb{N}}$  is a positive non-increasing sequence of real numbers satisfying the conditions*

$$\lim_k \epsilon_k = 0, \quad \sum_{k=1}^{\infty} \epsilon_k = \infty.$$

The step size  $\{\omega_k\}_{k \in \mathbb{N}}$  is a positive decreasing sequence of real numbers such that

$$\omega_k \rightarrow 0, \quad \sum_{k=1}^{\infty} \omega_k = +\infty, \quad \liminf_{k \rightarrow \infty} 2\phi \frac{\omega_k}{\omega_{k+1}} + \frac{\omega_{k+1} - \omega_k}{\omega_{k+1}^2} > 0. \quad (30)$$

According to [Benveniste et al. \[1990\]](#), we can choose  $\omega_k := \frac{A}{k^{\alpha+B}}$  for some  $\alpha \in (\frac{1}{2}, 1]$  and some suitable constants  $A > 0$  and  $B > 0$ .



**Theorem 3** ( $L^2$  convergence rate, restatement of Theorem 1). *Suppose Assumptions A1-A5 hold. For a sufficiently large value of  $m$ , a sufficiently small learning rate sequence  $\{\epsilon_k\}_{k=1}^\infty$ , and a sufficiently small step size sequence  $\{\omega_k\}_{k=1}^\infty$ ,  $\{\theta_k\}_{k=0}^\infty$  converges to  $\theta_*$  in  $L_2$ -norm such that*

$$\mathbb{E} [\|\theta_k - \theta_*\|^2] = \mathcal{O} \left( \omega_k + \sup_{i \geq k_0} \epsilon_i + \frac{1}{m} + \sup_{\mathbf{x}} \text{Var}(\xi_n(\mathbf{x})) \right),$$

where  $k_0$  is a sufficiently large constant,  $\xi_n$  is the noisy energy estimator of batch size  $n$ , and  $\text{Var}(\cdot)$  denotes the variance.

**Proof** Consider the iterations

$$\theta_{k+1} = \theta_k + \omega_{k+1} \left( \tilde{H}(\theta_k, \mathbf{x}_{k+1}) + \omega_{k+1} \rho(\theta_k, \mathbf{x}_{k+1}) \right).$$

Define  $\mathbf{T}_k = \theta_k - \theta_*$ . By subtracting  $\theta_*$  from both sides and taking the square and  $L_2$  norm, we have

$$\|\mathbf{T}_{k+1}\|^2 = \|\mathbf{T}_k\|^2 + \omega_{k+1}^2 \|\tilde{H}(\theta_k, \mathbf{x}_{k+1}) + \omega_{k+1} \rho(\theta_k, \mathbf{x}_{k+1})\|^2 + 2\omega_{k+1} \underbrace{\langle \mathbf{T}_k, \tilde{H}(\theta_k, \mathbf{x}_{k+1}) + \omega_{k+1} \rho(\theta_k, \mathbf{x}_{k+1}) \rangle}_{\text{D}}.$$

First, by Lemma 7, there exists a constant  $G = 4Q^2(1 + Q^2)$  such that

$$\|\tilde{H}(\theta_k, \mathbf{x}_{k+1}) + \omega_{k+1} \rho(\theta_k, \mathbf{x}_{k+1})\|^2 \leq G(1 + \|\mathbf{T}_k\|^2). \quad (31)$$

Next, by the Poisson equation (28), we have

$$\begin{aligned} \text{D} &= \langle \mathbf{T}_k, \tilde{H}(\theta_k, \mathbf{x}_{k+1}) + \omega_{k+1} \rho(\theta_k, \mathbf{x}_{k+1}) \rangle \\ &= \langle \mathbf{T}_k, h(\theta_k) + \mu_{\theta_k}(\mathbf{x}_{k+1}) - \Pi_{\theta_k} \mu_{\theta_k}(\mathbf{x}_{k+1}) + \omega_{k+1} \rho(\theta_k, \mathbf{x}_{k+1}) \rangle \\ &= \underbrace{\langle \mathbf{T}_k, h(\theta_k) \rangle}_{\text{D}_1} + \underbrace{\langle \mathbf{T}_k, \mu_{\theta_k}(\mathbf{x}_{k+1}) - \Pi_{\theta_k} \mu_{\theta_k}(\mathbf{x}_{k+1}) \rangle}_{\text{D}_2} + \underbrace{\langle \mathbf{T}_k, \omega_{k+1} \rho(\theta_k, \mathbf{x}_{k+1}) \rangle}_{\text{D}_3}. \end{aligned}$$

For the term  $\text{D}_1$ , by Lemma 3, we have

$$\mathbb{E} [\langle \mathbf{T}_k, h(\theta_k) \rangle] \leq -\phi \mathbb{E} [\|\mathbf{T}_k\|^2] + \mathcal{O}(\sup_{\mathbf{x}} \text{Var}(\xi_n(\mathbf{x})) + \epsilon_k + \frac{1}{m}).$$

For convenience, in the following context, we denote  $\mathcal{O}(\sup_{\mathbf{x}} \text{Var}(\xi_n(\mathbf{x})) + \epsilon_k + \frac{1}{m})$  by  $\Delta_k$ .

To deal with the term  $\text{D}_2$ , we make the following decomposition

$$\begin{aligned} \text{D}_2 &= \underbrace{\langle \mathbf{T}_k, \mu_{\theta_k}(\mathbf{x}_{k+1}) - \Pi_{\theta_k} \mu_{\theta_k}(\mathbf{x}_{k+1}) \rangle}_{\text{D}_{21}} \\ &\quad + \underbrace{\langle \mathbf{T}_k, \Pi_{\theta_k} \mu_{\theta_k}(\mathbf{x}_k) - \Pi_{\theta_{k-1}} \mu_{\theta_{k-1}}(\mathbf{x}_k) \rangle}_{\text{D}_{22}} + \underbrace{\langle \mathbf{T}_k, \Pi_{\theta_{k-1}} \mu_{\theta_{k-1}}(\mathbf{x}_k) - \Pi_{\theta_k} \mu_{\theta_k}(\mathbf{x}_{k+1}) \rangle}_{\text{D}_{23}}. \end{aligned}$$

(i) From the Markov property,  $\mu_{\theta_k}(\mathbf{x}_{k+1}) - \Pi_{\theta_k} \mu_{\theta_k}(\mathbf{x}_k)$  forms a martingale difference sequence

$$\mathbb{E} [\langle \mathbf{T}_k, \mu_{\theta_k}(\mathbf{x}_{k+1}) - \Pi_{\theta_k} \mu_{\theta_k}(\mathbf{x}_k) \rangle | \mathcal{F}_k] = 0, \quad (\text{D}_{21})$$

where  $\mathcal{F}_k$  is a  $\sigma$ -filter formed by  $\{\theta_0, \mathbf{x}_1, \theta_1, \mathbf{x}_2, \dots, \mathbf{x}_k, \theta_k\}$ .

(ii) By the regularity of the solution of Poisson equation in (29) and Lemma 8, we have

$$\mathbb{E} [\|\Pi_{\theta_k} \mu_{\theta_k}(\mathbf{x}_k) - \Pi_{\theta_{k-1}} \mu_{\theta_{k-1}}(\mathbf{x}_k)\|] \leq C \|\theta_k - \theta_{k-1}\| \leq 2QC\omega_k. \quad (32)$$

Using Cauchy–Schwarz inequality, (32) and the compactness of  $\Theta$  in Assumption A1, we have

$$\mathbb{E} [\langle \mathbf{T}_k, \Pi_{\theta_k} \mu_{\theta_k}(\mathbf{x}_k) - \Pi_{\theta_{k-1}} \mu_{\theta_{k-1}}(\mathbf{x}_k) \rangle] \leq \mathbb{E} [\|\mathbf{T}_k\|] \cdot 2QC\omega_k \leq 4Q^2C\omega_k \leq 5Q^2C\omega_{k+1} \quad (\text{D}_{22}),$$

where the last inequality follows from assumption A5 and holds for a large enough  $k$ .

(iii) For the last term of  $\text{D}_2$ ,

$$\begin{aligned} &\langle \mathbf{T}_k, \Pi_{\theta_{k-1}} \mu_{\theta_{k-1}}(\mathbf{x}_k) - \Pi_{\theta_k} \mu_{\theta_k}(\mathbf{x}_{k+1}) \rangle \\ &= (\langle \mathbf{T}_k, \Pi_{\theta_{k-1}} \mu_{\theta_{k-1}}(\mathbf{x}_k) \rangle - \langle \mathbf{T}_{k+1}, \Pi_{\theta_k} \mu_{\theta_k}(\mathbf{x}_{k+1}) \rangle) \\ &\quad + (\langle \mathbf{T}_{k+1}, \Pi_{\theta_k} \mu_{\theta_k}(\mathbf{x}_{k+1}) \rangle - \langle \mathbf{T}_k, \Pi_{\theta_k} \mu_{\theta_k}(\mathbf{x}_{k+1}) \rangle) \\ &= (z_k - z_{k+1}) + \langle \mathbf{T}_{k+1} - \mathbf{T}_k, \Pi_{\theta_k} \mu_{\theta_k}(\mathbf{x}_{k+1}) \rangle, \end{aligned}$$

where  $z_k = \langle \mathbf{T}_k, \Pi_{\boldsymbol{\theta}_{k-1}} \mu_{\boldsymbol{\theta}_{k-1}}(\mathbf{x}_k) \rangle$ . By the regularity assumption (29) and Lemma 8,

$$\mathbb{E} \langle \mathbf{T}_{k+1} - \mathbf{T}_k, \Pi_{\boldsymbol{\theta}_k} \mu_{\boldsymbol{\theta}_k}(\mathbf{x}_{k+1}) \rangle \leq \mathbb{E}[\|\boldsymbol{\theta}_{k+1} - \boldsymbol{\theta}_k\|] \cdot \mathbb{E}[\|\Pi_{\boldsymbol{\theta}_k} \mu_{\boldsymbol{\theta}_k}(\mathbf{x}_{k+1})\|] \leq 2QC\omega_{k+1}. \quad (\text{D}_{23})$$

Regarding  $\text{D}_3$ , since  $\rho(\boldsymbol{\theta}_k, \mathbf{x}_{k+1})$  is bounded, applying Cauchy–Schwarz inequality gives

$$\mathbb{E}[\langle \mathbf{T}_k, \omega_{k+1} \rho(\boldsymbol{\theta}_k, \mathbf{x}_{k+1}) \rangle] \leq 2Q^2\omega_{k+1} \quad (\text{D}_3)$$

Finally, adding (31),  $\text{D}_1$ ,  $\text{D}_{21}$ ,  $\text{D}_{22}$ ,  $\text{D}_{23}$  and  $\text{D}_3$  together, it follows that for a constant  $C_0 = G + 10Q^2C + 4QC + 4Q^2$ ,

$$\mathbb{E}[\|\mathbf{T}_{k+1}\|^2] \leq (1 - 2\omega_{k+1}\phi + G\omega_{k+1}^2)\mathbb{E}[\|\mathbf{T}_k\|^2] + C_0\omega_{k+1}^2 + 2\Delta_k\omega_{k+1} + 2\mathbb{E}[z_k - z_{k+1}]\omega_{k+1}. \quad (33)$$

Moreover, from (18) and (29),  $\mathbb{E}[|z_k|]$  is upper bounded by

$$\mathbb{E}[|z_k|] = \mathbb{E}[\langle \mathbf{T}_k, \Pi_{\boldsymbol{\theta}_{k-1}} \mu_{\boldsymbol{\theta}_{k-1}}(\mathbf{x}_k) \rangle] \leq \mathbb{E}[\|\mathbf{T}_k\|]\mathbb{E}[\|\Pi_{\boldsymbol{\theta}_{k-1}} \mu_{\boldsymbol{\theta}_{k-1}}(\mathbf{x}_k)\|] \leq 2QC. \quad (34)$$

According to Lemma 9, we can choose  $\lambda_0$  and  $k_0$  such that

$$\mathbb{E}[\|\mathbf{T}_{k_0}\|^2] \leq \psi_{k_0} = \lambda_0\omega_{k_0} + \frac{1}{\phi} \sup_{i \geq k_0} \Delta_i,$$

which satisfies the conditions (45) and (46) of Lemma 11. Applying Lemma 11 leads to

$$\mathbb{E}[\|\mathbf{T}_k\|^2] \leq \psi_k + \mathbb{E} \left[ \sum_{j=k_0+1}^k \Lambda_j^k (z_{j-1} - z_j) \right], \quad (35)$$

where  $\psi_k = \lambda_0\omega_k + \frac{1}{\phi} \sup_{i \geq k_0} \Delta_i$  for all  $k > k_0$ . Based on (34) and the increasing condition of  $\Lambda_j^k$  in Lemma 10, we have

$$\begin{aligned} & \mathbb{E} \left[ \sum_{j=k_0+1}^k \Lambda_j^k (z_{j-1} - z_j) \right] = \mathbb{E} \left[ \sum_{j=k_0+1}^{k-1} (\Lambda_{j+1}^k - \Lambda_j^k) z_j - 2\omega_k z_k + \Lambda_{k_0+1}^k z_{k_0} \right] \\ & \leq \sum_{j=k_0+1}^{k-1} 2(\Lambda_{j+1}^k - \Lambda_j^k)QC + \mathbb{E}[|2\omega_k z_k|] + 2\Lambda_{k_0+1}^k QC \\ & \leq 2(\Lambda_k^k - \Lambda_{k_0}^k)QC + 2\Lambda_k^k QC + 2\Lambda_{k_0}^k QC \\ & \leq 6\Lambda_k^k QC. \end{aligned} \quad (36)$$

Given  $\psi_k = \lambda_0\omega_k + \frac{1}{\phi} \sup_{i \geq k_0} \Delta_i$  which satisfies the conditions (45) and (46) of Lemma 11, it follows from (35) and (36) that the following inequality holds for any  $k > k_0$ ,

$$\mathbb{E}[\|\mathbf{T}_k\|^2] \leq \psi_k + 6\Lambda_k^k QC = (\lambda_0 + 12QC)\omega_k + \frac{1}{\phi} \sup_{i \geq k_0} \Delta_i = \lambda\omega_k + \frac{1}{\phi} \sup_{i \geq k_0} \Delta_i,$$

where  $\lambda = \lambda_0 + 12QC$ ,  $\lambda_0 = \frac{2G \sup_{i \geq k_0} \Delta_i + 2C_0\phi}{C_1\phi}$ ,  $C_1 = \liminf 2\phi \frac{\omega_k}{\omega_{k+1}} + \frac{\omega_{k+1} - \omega_k}{\omega_{k+1}^2} > 0$ ,  $C_0 = G + 5Q^2C + 2QC + 2Q^2$  and  $G = 4Q^2(1 + Q^2)$ .

### B.3 Technical lemmas

**Lemma 6.** *Suppose Assumption A1 holds, and  $u_1$  and  $u_{m-1}$  are fixed such that  $\Psi(u_1) > \nu$  and  $\Psi(u_{m-1}) > 1 - \nu$  for some small constant  $\nu > 0$ . For any bounded function  $f(\mathbf{x})$ , we have*

$$\int_{\mathcal{X}} f(\mathbf{x}) (\varpi_{\Psi_{\boldsymbol{\theta}}}(\mathbf{x}) - \varpi_{\tilde{\Psi}_{\boldsymbol{\theta}}}(\mathbf{x})) d\mathbf{x} = \mathcal{O}\left(\frac{1}{m}\right). \quad (37)$$

**Proof** Recall that  $\varpi_{\tilde{\Psi}_\theta}(\mathbf{x}) = \frac{1}{Z_\theta} \frac{\pi(\mathbf{x})}{\theta^\zeta(J(\mathbf{x}))}$  and  $\varpi_{\Psi_\theta}(\mathbf{x}) = \frac{1}{Z_{\Psi_\theta}} \frac{\pi(\mathbf{x})}{\Psi_\theta^\zeta(U(\mathbf{x}))}$ . Since  $f(\mathbf{x})$  is bounded, it suffices to show

$$\begin{aligned} & \int_{\mathcal{X}} \frac{1}{Z_\theta} \frac{\pi(\mathbf{x})}{\theta^\zeta(J(\mathbf{x}))} - \frac{1}{Z_{\Psi_\theta}} \frac{\pi(\mathbf{x})}{\Psi_\theta^\zeta(U(\mathbf{x}))} d\mathbf{x} \\ & \leq \int_{\mathcal{X}} \left| \frac{1}{Z_\theta} \frac{\pi(\mathbf{x})}{\theta^\zeta(J(\mathbf{x}))} - \frac{1}{Z_\theta} \frac{\pi(\mathbf{x})}{\Psi_\theta^\zeta(U(\mathbf{x}))} \right| d\mathbf{x} + \int_{\mathcal{X}} \left| \frac{1}{Z_\theta} \frac{\pi(\mathbf{x})}{\Psi_\theta^\zeta(U(\mathbf{x}))} - \frac{1}{Z_{\Psi_\theta}} \frac{\pi(\mathbf{x})}{\Psi_\theta^\zeta(U(\mathbf{x}))} \right| d\mathbf{x} \quad (38) \\ & = \underbrace{\frac{1}{Z_\theta} \sum_{i=1}^m \int_{\mathcal{X}_i} \left| \frac{\pi(\mathbf{x})}{\theta^\zeta(i)} - \frac{\pi(\mathbf{x})}{\Psi_\theta^\zeta(U(\mathbf{x}))} \right| d\mathbf{x}}_{I_1} + \underbrace{\sum_{i=1}^m \left| \frac{1}{Z_\theta} - \frac{1}{Z_{\Psi_\theta}} \right| \int_{\mathcal{X}_i} \frac{\pi(\mathbf{x})}{\Psi_\theta^\zeta(U(\mathbf{x}))} d\mathbf{x}}_{I_2} = \mathcal{O}\left(\frac{1}{m}\right), \end{aligned}$$

where  $Z_\theta = \sum_{i=1}^m \int_{\mathcal{X}_i} \frac{\pi(\mathbf{x})}{\theta(i)^\zeta} d\mathbf{x}$ ,  $Z_{\Psi_\theta} = \sum_{i=1}^m \int_{\mathcal{X}_i} \frac{\pi(\mathbf{x})}{\Psi_\theta^\zeta(U(\mathbf{x}))} d\mathbf{x}$ , and  $\Psi_\theta(u)$  is a piecewise continuous function defined in (21).

By Assumption A1,  $\inf_{\Theta} \theta(i) > 0$  for any  $i$ . Further, by the mean-value theorem, which implies  $|x^\zeta - y^\zeta| \lesssim |x - y|z^\zeta$  for any  $\zeta > 0$ ,  $x \leq y$  and  $z \in [x, y] \subset [u_1, \infty)$ , we have

$$\begin{aligned} I_1 &= \frac{1}{Z_\theta} \sum_{i=1}^m \int_{\mathcal{X}_i} \left| \frac{\theta^\zeta(i) - \Psi_\theta^\zeta(U(\mathbf{x}))}{\theta^\zeta(i)\Psi_\theta^\zeta(U(\mathbf{x}))} \right| \pi(\mathbf{x}) d\mathbf{x} \lesssim \frac{1}{Z_\theta} \sum_{i=1}^m \int_{\mathcal{X}_i} \frac{|\Psi_\theta(u_{i-1}) - \Psi_\theta(u_i)|}{\theta^\zeta(i)} \pi(\mathbf{x}) d\mathbf{x} \\ &\leq \max_i |\Psi_\theta(u_i - \Delta u) - \Psi_\theta(u_i)| \frac{1}{Z_\theta} \sum_{i=1}^m \int_{\mathcal{X}_i} \frac{\pi(\mathbf{x})}{\theta^\zeta(i)} d\mathbf{x} = \max_i |\Psi_\theta(u_i - \Delta u) - \Psi_\theta(u_i)| \lesssim \Delta u = \mathcal{O}\left(\frac{1}{m}\right), \end{aligned}$$

where the last inequality follows by Taylor expansion, and the last equality follows as  $u_1$  and  $u_{m-1}$  are fixed. Similarly, we have

$$I_2 = \left| \frac{1}{Z_\theta} - \frac{1}{Z_{\Psi_\theta}} \right| Z_{\Psi_\theta} = \frac{|Z_{\Psi_\theta} - Z_\theta|}{Z_\theta} \leq \frac{1}{Z_\theta} \sum_{i=1}^m \int_{\mathcal{X}_i} \left| \frac{\pi(\mathbf{x})}{\theta^\zeta(i)} - \frac{\pi(\mathbf{x})}{\Psi_\theta^\zeta(U(\mathbf{x}))} \right| d\mathbf{x} = I_1 = \mathcal{O}\left(\frac{1}{m}\right).$$

The proof can then be concluded by combining the orders of  $I_1$  and  $I_2$ .

**Lemma 7.** Given  $\sup\{\omega_k\}_{k=1}^\infty \leq 1$ , there exists a constant  $G = 4Q^2(1 + Q^2)$  such that

$$\|\tilde{H}(\boldsymbol{\theta}_k, \mathbf{x}_{k+1}) + \omega_{k+1}\rho(\boldsymbol{\theta}_k, \mathbf{x}_{k+1})\|^2 \leq G(1 + \|\boldsymbol{\theta}_k - \boldsymbol{\theta}_*\|^2). \quad (39)$$

**Proof**

According to the compactness condition in Assumption A1, we have

$$\|\tilde{H}(\boldsymbol{\theta}_k, \mathbf{x}_{k+1})\|^2 \leq Q^2(1 + \|\boldsymbol{\theta}_k\|^2) = Q^2(1 + \|\boldsymbol{\theta}_k - \boldsymbol{\theta}_* + \boldsymbol{\theta}_*\|^2) \leq Q^2(1 + 2\|\boldsymbol{\theta}_k - \boldsymbol{\theta}_*\|^2 + 2Q^2). \quad (40)$$

Therefore, using (40), we can show that for a constant  $G = 4Q^2(1 + Q^2)$

$$\begin{aligned} & \|\tilde{H}(\boldsymbol{\theta}_k, \mathbf{x}_{k+1}) + \omega_{k+1}\rho(\boldsymbol{\theta}_k, \mathbf{x}_{k+1})\|^2 \\ & \leq 2\|\tilde{H}(\boldsymbol{\theta}_k, \mathbf{x}_{k+1})\|^2 + 2\omega_{k+1}^2\|\rho(\boldsymbol{\theta}_k, \mathbf{x}_{k+1})\|^2 \\ & \leq 2Q^2(1 + 2\|\boldsymbol{\theta}_k - \boldsymbol{\theta}_*\|^2 + 2Q^2) + 2Q^2 \\ & \leq 2Q^2(2 + 2Q^2 + (2 + 2Q^2)\|\boldsymbol{\theta}_k - \boldsymbol{\theta}_*\|^2) \\ & \leq G(1 + \|\boldsymbol{\theta}_k - \boldsymbol{\theta}_*\|^2). \end{aligned}$$

**Lemma 8.** Given  $\sup\{\omega_k\}_{k=1}^\infty \leq 1$ , we have that

$$\|\boldsymbol{\theta}_k - \boldsymbol{\theta}_{k-1}\| \leq 2\omega_k Q \quad (41)$$

**Proof** Following the update  $\boldsymbol{\theta}_k - \boldsymbol{\theta}_{k-1} = \omega_k \tilde{H}(\boldsymbol{\theta}_{k-1}, \mathbf{x}_k) + \omega_k^2 \rho(\boldsymbol{\theta}_{k-1}, \mathbf{x}_k)$ , we have that

$$\|\boldsymbol{\theta}_k - \boldsymbol{\theta}_{k-1}\| = \|\omega_k \tilde{H}(\boldsymbol{\theta}_{k-1}, \mathbf{x}_k) + \omega_k^2 \rho(\boldsymbol{\theta}_{k-1}, \mathbf{x}_k)\| \leq \omega_k \|\tilde{H}(\boldsymbol{\theta}_{k-1}, \mathbf{x}_k)\| + \omega_k^2 \|\rho(\boldsymbol{\theta}_{k-1}, \mathbf{x}_k)\|.$$

By the compactness condition in Assumption A1 and  $\sup\{\omega_k\}_{k=1}^\infty \leq 1$ , (41) can be derived.

**Lemma 9.** *There exist constants  $\lambda_0$  and  $k_0$  such that  $\forall \lambda \geq \lambda_0$  and  $\forall k > k_0$ , the sequence  $\{\psi_k\}_{k=1}^\infty$ , where  $\psi_k = \lambda\omega_k + \frac{1}{\phi} \sup_{i \geq k_0} \Delta_i$ , satisfies*

$$\psi_{k+1} \geq (1 - 2\omega_{k+1}\phi + G\omega_{k+1}^2)\psi_k + C_0\omega_{k+1}^2 + 2\Delta_k\omega_{k+1}. \quad (42)$$

**Proof** By replacing  $\psi_k$  with  $\lambda\omega_k + \frac{1}{\phi} \sup_{i \geq k_0} \Delta_i$  in (42), it suffices to show

$$\lambda\omega_{k+1} + \frac{1}{\phi} \sup_{i \geq k_0} \Delta_i \geq (1 - 2\omega_{k+1}\phi + G\omega_{k+1}^2) \left( \lambda\omega_k + \frac{1}{\phi} \sup_{i \geq k_0} \Delta_i \right) + C_0\omega_{k+1}^2 + 2\Delta_k\omega_{k+1}.$$

which is equivalent to proving

$$\lambda(\omega_{k+1} - \omega_k + 2\omega_k\omega_{k+1}\phi - G\omega_k\omega_{k+1}^2) \geq \frac{1}{\phi} \sup_{i \geq k_0} \Delta_i (-2\omega_{k+1}\phi + G\omega_{k+1}^2) + C_0\omega_{k+1}^2 + 2\Delta_k\omega_{k+1}.$$

Given the step size condition in (30), we have

$$\omega_{k+1} - \omega_k + 2\omega_k\omega_{k+1}\phi \geq C_1\omega_{k+1}^2,$$

where  $C_1 = \liminf 2\phi \frac{\omega_k}{\omega_{k+1}} + \frac{\omega_{k+1} - \omega_k}{\omega_{k+1}^2} > 0$ . Combining  $-\sup_{i \geq k_0} \Delta_i \leq \Delta_k$ , it suffices to prove

$$\lambda(C_1 - G\omega_k)\omega_{k+1}^2 \geq \left( \frac{G}{\phi} \sup_{i \geq k_0} \Delta_i + C_0 \right) \omega_{k+1}^2. \quad (43)$$

It is clear that for a large enough  $k_0$  and  $\lambda_0$  such that  $\omega_{k_0} \leq \frac{C_1}{2G}$ ,  $\lambda_0 = \frac{2G \sup_{i \geq k_0} \Delta_i + 2C_0\phi}{C_1\phi}$ , the desired conclusion (43) holds for all such  $k \geq k_0$  and  $\lambda \geq \lambda_0$ .

The following lemma is a restatement of Lemma 25 (page 247) from Benveniste et al. [1990].

**Lemma 10.** *Suppose  $k_0$  is an integer satisfying  $\inf_{k > k_0} \frac{\omega_{k+1} - \omega_k}{\omega_k\omega_{k+1}} + 2\phi - G\omega_{k+1} > 0$  for some constant  $G$ . Then for any  $k > k_0$ , the sequence  $\{\Lambda_k^K\}_{k=k_0, \dots, K}$  defined below is increasing and upper bounded by  $2\omega_k$*

$$\Lambda_k^K = \begin{cases} 2\omega_k \prod_{j=k}^{K-1} (1 - 2\omega_{j+1}\phi + G\omega_{j+1}^2) & \text{if } k < K, \\ 2\omega_k & \text{if } k = K. \end{cases} \quad (44)$$

**Lemma 11.** *Let  $\{\psi_k\}_{k > k_0}$  be a series that satisfies the following inequality for all  $k > k_0$*

$$\psi_{k+1} \geq \psi_k (1 - 2\omega_{k+1}\phi + G\omega_{k+1}^2) + C_0\omega_{k+1}^2 + 2\Delta_k\omega_{k+1}, \quad (45)$$

and assume there exists such  $k_0$  that

$$\mathbb{E} [\|\mathbf{T}_{k_0}\|^2] \leq \psi_{k_0}. \quad (46)$$

Then for all  $k > k_0$ , we have

$$\mathbb{E} [\|\mathbf{T}_k\|^2] \leq \psi_k + \sum_{j=k_0+1}^k \Lambda_j^k (z_{j-1} - z_j). \quad (47)$$

**Proof** We prove by the induction method. Assuming (47) is true and applying (33), we have that

$$\begin{aligned} \mathbb{E} [\|\mathbf{T}_{k+1}\|^2] &\leq (1 - 2\omega_{k+1}\phi + \omega_{k+1}^2 G) (\psi_k + \sum_{j=k_0+1}^k \Lambda_j^k (z_{j-1} - z_j)) \\ &\quad + C_0\omega_{k+1}^2 + 2\Delta_k\omega_{k+1} + 2\omega_{k+1}\mathbb{E}[z_k - z_{k+1}] \end{aligned}$$

Combining (42) and Lemma.10, respectively, we have

$$\begin{aligned} \mathbb{E} [\|\mathbf{T}_{k+1}\|^2] &\leq \psi_{k+1} + (1 - 2\omega_{k+1}\phi + \omega_{k+1}^2 G) \sum_{j=k_0+1}^k \Lambda_j^k (z_{j-1} - z_j) + 2\omega_{k+1}\mathbb{E}[z_k - z_{k+1}] \\ &\leq \psi_{k+1} + \sum_{j=k_0+1}^k \Lambda_j^{k+1} (z_{j-1} - z_j) + \Lambda_{k+1}^{k+1} \mathbb{E}[z_k - z_{k+1}] \\ &\leq \psi_{k+1} + \sum_{j=k_0+1}^{k+1} \Lambda_j^{k+1} (z_{j-1} - z_j). \end{aligned}$$

## C Ergodicity and dynamic importance sampler

Our interest is to analyze the deviation between the weighted averaging estimator  $\frac{1}{k} \sum_{i=1}^k \theta_i^s (J_{\tilde{U}}(\mathbf{x}_i)) f(\mathbf{x}_i)$  and posterior expectation  $\int_{\mathcal{X}} f(\mathbf{x}) \pi(d\mathbf{x})$  for a bounded function  $f$ . To accomplish this analysis, we first study the convergence of the posterior sample mean  $\frac{1}{k} \sum_{i=1}^k f(\mathbf{x}_i)$  to the posterior expectation  $\bar{f} = \int_{\mathcal{X}} f(\mathbf{x}) \varpi_{\Psi_{\theta_*}}(\mathbf{x})(d\mathbf{x})$  and then extend it to  $\int_{\mathcal{X}} f(\mathbf{x}) \varpi_{\tilde{\Psi}_{\theta_*}}(\mathbf{x})(d\mathbf{x})$ . The key tool for establishing the ergodic theory is still the Poisson equation which is used to characterize the fluctuation between  $f(\mathbf{x})$  and  $\bar{f}$ :

$$\mathcal{L}g(\mathbf{x}) = f(\mathbf{x}) - \bar{f}, \quad (48)$$

where  $g(\mathbf{x})$  is the solution of the Poisson equation, and  $\mathcal{L}$  is the infinitesimal generator of the Langevin diffusion

$$\mathcal{L}g := \langle \nabla g, \nabla L(\cdot, \boldsymbol{\theta}_*) \rangle + \tau \nabla^2 g.$$

To control the perturbations of  $\frac{1}{k} \sum_{i=1}^k f(\mathbf{x}_i) - \bar{f}$  and enables convergence of the weighted averaging estimate, [Chen et al. \[2015\]](#) impose the following regularity conditions on the solution  $g(\mathbf{x})$ :

**Regularity** Given a sufficiently smooth function  $g(\mathbf{x})$  and a function  $\mathcal{V}(\mathbf{x})$  such that  $\|D^k g\| \lesssim \mathcal{V}^{p_k}(\mathbf{x})$  for some constants  $p_k > 0$ , where  $k \in \{0, 1, 2, 3\}$ . In addition,  $\mathcal{V}^p$  has a bounded expectation, i.e.,  $\sup_{\mathbf{x}} \mathbb{E}[\mathcal{V}^p(\mathbf{x})] < \infty$ ; and  $\mathcal{V}$  is smooth, i.e.  $\sup_{s \in \{0,1\}} \mathcal{V}^p(s\mathbf{x} + (1-s)\mathbf{y}) \lesssim \mathcal{V}^p(\mathbf{x}) + \mathcal{V}^p(\mathbf{y})$  for all  $\mathbf{x}, \mathbf{y} \in \mathcal{X}$  and  $p \leq 2 \max_k \{p_k\}$ .

For stronger but verifiable conditions, we refer readers to [Vollmer et al. \[2016\]](#). For further verifications, [Erdogdu et al. \[2018\]](#) showed that the 0th, 1st and 2nd order of the regularity can be verified given standard smoothness and dissipative assumptions. In what follows, we present a lemma, which is majorly adapted from Theorem 2 of [Chen et al. \[2015\]](#) with a fixed learning rate  $\epsilon$ .

**Lemma 12** (Convergence of the Averaging Estimators, restatement of Lemma 2). *Suppose Assumptions A1-A5 hold. For any bounded function  $f$ ,*

$$\left| \mathbb{E} \left[ \frac{\sum_{i=1}^k f(\mathbf{x}_i)}{k} \right] - \int_{\mathcal{X}} f(\mathbf{x}) \varpi_{\tilde{\Psi}_{\theta_*}}(\mathbf{x}) d\mathbf{x} \right| = \mathcal{O} \left( \frac{1}{k\epsilon} + \sqrt{\epsilon} + \sqrt{\frac{\sum_{i=1}^k \omega_i}{k}} + \frac{1}{\sqrt{m}} + \sqrt{\sup_{\mathbf{x}} \text{Var}(\xi_n(\mathbf{x}))} \right),$$

where  $k_0$  is a sufficiently large constant,  $\varpi_{\tilde{\Psi}_{\theta_*}}(\mathbf{x}) \propto \frac{\pi(\mathbf{x})}{\theta_*^s(J(\mathbf{x}))}$ , and  $\frac{\sum_{i=1}^k \omega_i}{k} = o(\frac{1}{\sqrt{k}})$  as implied by Assumption A5.

**Proof** We rewrite the CSGLD algorithm as follows:

$$\begin{aligned} \mathbf{x}_{k+1} &= \mathbf{x}_k - \epsilon_k \nabla_{\mathbf{x}} \tilde{L}(\mathbf{x}_k, \boldsymbol{\theta}_k) + \mathcal{N}(0, 2\epsilon_k \tau \mathbf{I}) \\ &= \mathbf{x}_k - \epsilon_k \left( \nabla_{\mathbf{x}} \hat{L}(\mathbf{x}_k, \boldsymbol{\theta}_*) + \Upsilon(\mathbf{x}_k, \boldsymbol{\theta}_k, \boldsymbol{\theta}_*) \right) + \mathcal{N}(0, 2\epsilon_k \tau \mathbf{I}), \end{aligned}$$

where  $\nabla_{\mathbf{x}} \hat{L}(\mathbf{x}, \boldsymbol{\theta}) = \frac{N}{n} \left[ 1 + \frac{\zeta \tau}{\Delta u} (\log \theta(J(\mathbf{x})) - \log \theta((J(\mathbf{x}) - 1) \vee 1)) \right] \nabla_{\mathbf{x}} \tilde{U}(\mathbf{x})$ ,  $\nabla_{\mathbf{x}} \tilde{L}(\mathbf{x}, \boldsymbol{\theta})$  is as defined in Section B.1, and the bias term is given by  $\Upsilon(\mathbf{x}_k, \boldsymbol{\theta}_k, \boldsymbol{\theta}_*) = \nabla_{\mathbf{x}} \tilde{L}(\mathbf{x}_k, \boldsymbol{\theta}_k) - \nabla_{\mathbf{x}} \hat{L}(\mathbf{x}_k, \boldsymbol{\theta}_*)$ .

By Assumption A2, we have  $\|\nabla_{\mathbf{x}} U(\mathbf{x})\| = \|\nabla_{\mathbf{x}} U(\mathbf{x}) - \nabla_{\mathbf{x}} U(\mathbf{x}_*)\| \lesssim \|\mathbf{x} - \mathbf{x}_*\| \leq \|\mathbf{x}\| + \|\mathbf{x}_*\|$  for some optimum. Then the  $L^2$  upper bound in Lemma 4 implies that  $\nabla_{\mathbf{x}} U(\mathbf{x})$  has a bounded second moment. Combining Assumption A4, we have  $\mathbb{E} \left[ \|\nabla_{\mathbf{x}} \tilde{U}(\mathbf{x})\|^2 \right] < \infty$ . Further by Eve's law (i.e., the variance decomposition formula), it is easy to derive that  $\mathbb{E} \left[ \|\nabla_{\mathbf{x}} \tilde{U}(\mathbf{x})\| \right] < \infty$ . Then, by the triangle inequality and Jensen's inequality,

$$\begin{aligned} \|\mathbb{E}[\Upsilon(\mathbf{x}_k, \boldsymbol{\theta}_k, \boldsymbol{\theta}_*)]\| &\leq \mathbb{E}[\|\nabla_{\mathbf{x}} \tilde{L}(\mathbf{x}_k, \boldsymbol{\theta}_k) - \nabla_{\mathbf{x}} \tilde{L}(\mathbf{x}_k, \boldsymbol{\theta}_*)\|] + \mathbb{E}[\|\nabla_{\mathbf{x}} \tilde{L}(\mathbf{x}_k, \boldsymbol{\theta}_*) - \nabla_{\mathbf{x}} \hat{L}(\mathbf{x}_k, \boldsymbol{\theta}_*)\|] \\ &\leq \mathbb{E}[\|\boldsymbol{\theta}_k - \boldsymbol{\theta}_*\|] + \mathcal{O}(\sup_{\mathbf{x}} \text{Var}(\xi_n(\mathbf{x}))) \leq \sqrt{\mathbb{E}[\|\boldsymbol{\theta}_k - \boldsymbol{\theta}_*\|^2]} + \mathcal{O}(\sup_{\mathbf{x}} \text{Var}(\xi_n(\mathbf{x}))) \\ &\leq \mathcal{O} \left( \sqrt{\omega_k + \epsilon + \frac{1}{m} + \sup_{\mathbf{x}} \text{Var}(\xi_n(\mathbf{x}))} \right), \end{aligned} \quad (49)$$

where Assumption A1 and Theorem 3 are used to derive the smoothness of  $\nabla_{\mathbf{x}} \tilde{L}(\mathbf{x}, \boldsymbol{\theta})$  with respect to  $\boldsymbol{\theta}$ , and  $\sup_{\mathbf{x}} \text{Var}(\xi_n(\mathbf{x}))$  is the bias caused by the mini-batch evaluation of  $U(\mathbf{x})$ .

The ergodic average based on biased gradients and a fixed learning rate is a direct result of Theorem 2 of Chen et al. [2015]. By simulating from  $\varpi_{\Psi_{\theta_*}}(\mathbf{x}) \propto \frac{\pi(\mathbf{x})}{\Psi_{\theta_*}^{\zeta}(U(\mathbf{x}))}$  and combining (49) and Theorem 3, we have

$$\begin{aligned} \left| \mathbb{E} \left[ \frac{\sum_{i=1}^k f(\mathbf{x}_i)}{k} \right] - \int_{\mathcal{X}} f(\mathbf{x}) \varpi_{\Psi_{\theta_*}}(\mathbf{x}) d\mathbf{x} \right| &\leq \mathcal{O} \left( \frac{1}{k\epsilon} + \epsilon + \frac{\sum_{i=1}^k \|\mathbb{E}[\Upsilon(\mathbf{x}_k, \boldsymbol{\theta}_k, \boldsymbol{\theta}_*)]\|}{k} \right) \\ &\lesssim \mathcal{O} \left( \frac{1}{k\epsilon} + \epsilon + \frac{\sum_{i=1}^k \sqrt{\omega_i + \epsilon + \frac{1}{m} + \sup_{\mathbf{x}} \text{Var}(\xi_n(\mathbf{x}))}}{k} \right) \\ &\leq \mathcal{O} \left( \frac{1}{k\epsilon} + \sqrt{\epsilon} + \sqrt{\frac{\sum_{i=1}^k \omega_i}{k}} + \frac{1}{\sqrt{m}} + \sqrt{\sup_{\mathbf{x}} \text{Var}(\xi_n(\mathbf{x}))} \right), \end{aligned}$$

where the last inequality follows by repeatedly applying the inequality  $\sqrt{a+b} \leq \sqrt{a} + \sqrt{b}$  and the inequality  $\sum_{i=1}^k \sqrt{\omega_i} \leq \sqrt{k \sum_{i=1}^k \omega_i}$ .

For any a bounded function  $f(\mathbf{x})$ , we have  $|\int_{\mathcal{X}} f(\mathbf{x}) \varpi_{\Psi_{\theta_*}}(\mathbf{x}) d\mathbf{x} - \int_{\mathcal{X}} f(\mathbf{x}) \varpi_{\tilde{\Psi}_{\theta_*}}(\mathbf{x}) d\mathbf{x}| = \mathcal{O}(\frac{1}{m})$  by Lemma 6. By the triangle inequality, we have

$$\left| \mathbb{E} \left[ \frac{\sum_{i=1}^k f(\mathbf{x}_i)}{k} \right] - \int_{\mathcal{X}} f(\mathbf{x}) \varpi_{\tilde{\Psi}_{\theta_*}}(\mathbf{x}) d\mathbf{x} \right| \leq \mathcal{O} \left( \frac{1}{k\epsilon} + \sqrt{\epsilon} + \sqrt{\frac{\sum_{i=1}^k \omega_i}{k}} + \frac{1}{\sqrt{m}} + \sqrt{\sup_{\mathbf{x}} \text{Var}(\xi_n(\mathbf{x}))} \right),$$

which concludes the proof.

Finally, we are ready to show the convergence of the weighted averaging estimator  $\frac{\sum_{i=1}^k \theta_i^{\zeta}(J_{\bar{U}}(\mathbf{x}_i)) f(\mathbf{x}_i)}{\sum_{i=1}^k \theta_i^{\zeta}(J_{\bar{U}}(\mathbf{x}_i))}$  to the posterior mean  $\int_{\mathcal{X}} f(\mathbf{x}) \pi(d\mathbf{x})$ .

**Theorem 4** (Convergence of the Weighted Averaging Estimators, restatement of Theorem 2). *Assume Assumptions A1-A5 hold. For any bounded function  $f$ , we have that*

$$\left| \mathbb{E} \left[ \frac{\sum_{i=1}^k \theta_i^{\zeta}(J_{\bar{U}}(\mathbf{x}_i)) f(\mathbf{x}_i)}{\sum_{i=1}^k \theta_i^{\zeta}(J_{\bar{U}}(\mathbf{x}_i))} \right] - \int_{\mathcal{X}} f(\mathbf{x}) \pi(d\mathbf{x}) \right| = \mathcal{O} \left( \frac{1}{k\epsilon} + \sqrt{\epsilon} + \sqrt{\frac{\sum_{i=1}^k \omega_i}{k}} + \frac{1}{\sqrt{m}} + \sqrt{\sup_{\mathbf{x}} \text{Var}(\xi_n(\mathbf{x}))} \right).$$

## Proof

Applying triangle inequality and  $|\mathbb{E}[x]| \leq \mathbb{E}[|x|]$ , we have

$$\begin{aligned} &\left| \mathbb{E} \left[ \frac{\sum_{i=1}^k \theta_i^{\zeta}(J_{\bar{U}}(\mathbf{x}_i)) f(\mathbf{x}_i)}{\sum_{i=1}^k \theta_i^{\zeta}(J_{\bar{U}}(\mathbf{x}_i))} \right] - \int_{\mathcal{X}} f(\mathbf{x}) \pi(d\mathbf{x}) \right| \\ &\leq \underbrace{\mathbb{E} \left[ \left| \frac{\sum_{i=1}^k \theta_i^{\zeta}(J_{\bar{U}}(\mathbf{x}_i)) f(\mathbf{x}_i)}{\sum_{i=1}^k \theta_i^{\zeta}(J_{\bar{U}}(\mathbf{x}_i))} - \frac{\sum_{i=1}^k \theta_i^{\zeta}(J(\mathbf{x}_i)) f(\mathbf{x}_i)}{\sum_{i=1}^k \theta_i^{\zeta}(J(\mathbf{x}_i))} \right| \right]}_{I_1} \\ &\quad + \underbrace{\mathbb{E} \left[ \left| \frac{\sum_{i=1}^k \theta_i^{\zeta}(J(\mathbf{x}_i)) f(\mathbf{x}_i)}{\sum_{i=1}^k \theta_i^{\zeta}(J(\mathbf{x}_i))} - \frac{Z_{\theta_*} \sum_{i=1}^k \theta_i^{\zeta}(J(\mathbf{x}_i)) f(\mathbf{x}_i)}{k} \right| \right]}_{I_2} \\ &\quad + \underbrace{\mathbb{E} \left[ \frac{Z_{\theta_*}}{k} \sum_{i=1}^k \left| \theta_i^{\zeta}(J(\mathbf{x}_i)) - \theta_*^{\zeta}(J(\mathbf{x}_i)) \right| \cdot |f(\mathbf{x}_i)| \right]}_{I_3} + \underbrace{\left| \mathbb{E} \left[ \frac{Z_{\theta_*}}{k} \sum_{i=1}^k \theta_*^{\zeta}(J(\mathbf{x}_i)) f(\mathbf{x}_i) \right] - \int_{\mathcal{X}} f(\mathbf{x}) \pi(d\mathbf{x}) \right|}_{I_4}. \end{aligned}$$

For the term  $I_1$ , consider the bias  $\mathbb{E}[\tilde{H}(\boldsymbol{\theta}, \mathbf{x}) - H(\boldsymbol{\theta}, \mathbf{x})] = O(\sup_{\mathbf{x}} \text{Var}(\xi_n(\mathbf{x})))$  as defined in the proof of Lemma 3. By applying mean-value theorem, we have

$$\begin{aligned} I_1 &= \mathbb{E} \left[ \left| \frac{\left( \sum_{i=1}^k \theta_i^\zeta(J_{\bar{U}}(\mathbf{x}_i)) f(\mathbf{x}_i) \right) \left( \sum_{i=1}^k \theta_i^\zeta(J(\mathbf{x}_i)) \right) - \left( \sum_{i=1}^k \theta_i^\zeta(J(\mathbf{x}_i)) f(\mathbf{x}_i) \right) \left( \sum_{i=1}^k \theta_i^\zeta(J_{\bar{U}}(\mathbf{x}_i)) \right)}{\left( \sum_{i=1}^k \theta_i^\zeta(J_{\bar{U}}(\mathbf{x}_i)) \right) \left( \sum_{i=1}^k \theta_i^\zeta(J(\mathbf{x}_i)) \right)} \right| \right] \\ &\lesssim O\left(\sup_{\mathbf{x}} \text{Var}(\xi_n(\mathbf{x}))\right) \mathbb{E} \left[ \frac{\left( \sum_{i=1}^k \theta_i^\zeta(J(\mathbf{x}_i)) f(\mathbf{x}_i) \right) \left( \sum_{i=1}^k \theta_i^\zeta(J(\mathbf{x}_i)) \right)}{\left( \sum_{i=1}^k \theta_i^\zeta(J(\mathbf{x}_i)) \right) \left( \sum_{i=1}^k \theta_i^\zeta(J(\mathbf{x}_i)) \right)} \right] = O\left(\sup_{\mathbf{x}} \text{Var}(\xi_n(\mathbf{x}))\right). \end{aligned} \quad (50)$$

For the term  $I_2$ , by the boundedness of  $\Theta$  and  $f$  and the assumption  $\inf_{\Theta} \theta^\zeta(i) > 0$ , we have

$$\begin{aligned} I_2 &= \mathbb{E} \left[ \left| \frac{\sum_{i=1}^k \theta_i^\zeta(J(\mathbf{x}_i)) f(\mathbf{x}_i)}{\sum_{i=1}^k \theta_i^\zeta(J(\mathbf{x}_i))} \left( 1 - \sum_{i=1}^k \frac{\theta_i^\zeta(J(\mathbf{x}_i))}{k} Z_{\boldsymbol{\theta}_*} \right) \right| \right] \\ &\lesssim \mathbb{E} \left[ \left| Z_{\boldsymbol{\theta}_*} \frac{\sum_{i=1}^k \theta_i^\zeta(J(\mathbf{x}_i))}{k} - 1 \right| \right] \\ &= \mathbb{E} \left[ \left| Z_{\boldsymbol{\theta}_*} \sum_{i=1}^m \frac{\sum_{j=1}^k \left( \theta_j^\zeta(i) - \theta_*^\zeta(i) + \theta_*^\zeta(i) \right) 1_{J(\mathbf{x}_j)=i}}{k} - 1 \right| \right] \\ &\leq \underbrace{\mathbb{E} \left[ \left| Z_{\boldsymbol{\theta}_*} \sum_{i=1}^m \frac{\sum_{j=1}^k \left| \theta_j^\zeta(i) - \theta_*^\zeta(i) \right| 1_{J(\mathbf{x}_j)=i}}{k} \right| \right]}_{I_{21}} + \underbrace{\mathbb{E} \left[ \left| Z_{\boldsymbol{\theta}_*} \sum_{i=1}^m \frac{\theta_*^\zeta(i) \sum_{j=1}^k 1_{J(\mathbf{x}_j)=i}}{k} - 1 \right| \right]}_{I_{22}}. \end{aligned}$$

For  $I_{21}$ , by first applying the inequality  $|x^\zeta - y^\zeta| \leq \zeta |x - y| z^{\zeta-1}$  for any  $\zeta > 0$ ,  $x \leq y$  and  $z \in [x, y]$  based on the mean-value theorem and then applying the Cauchy-Schwarz inequality, we have

$$I_{21} \lesssim \frac{1}{k} \mathbb{E} \left[ \sum_{j=1}^k \sum_{i=1}^m \left| \theta_j^\zeta(i) - \theta_*^\zeta(i) \right| \right] \lesssim \frac{1}{k} \mathbb{E} \left[ \sum_{j=1}^k \sum_{i=1}^m \left| \theta_j(i) - \theta_*(i) \right| \right] \lesssim \frac{1}{k} \sqrt{\sum_{j=1}^k \mathbb{E} \left[ \|\boldsymbol{\theta}_j - \boldsymbol{\theta}_*\|^2 \right]}, \quad (51)$$

where the compactness of  $\Theta$  has been used in deriving the second inequality.

For  $I_{22}$ , considering the following relation

$$1 = \sum_{i=1}^m \int_{\mathcal{X}_i} \pi(\mathbf{x}) d\mathbf{x} = \sum_{i=1}^m \int_{\mathcal{X}_i} \theta_*^\zeta(i) \frac{\pi(\mathbf{x})}{\theta_*^\zeta(i)} d\mathbf{x} = Z_{\boldsymbol{\theta}_*} \int_{\mathcal{X}} \sum_{i=1}^m \theta_*^\zeta(i) 1_{J(\mathbf{x})=i} \varpi_{\tilde{\Psi}_{\boldsymbol{\theta}_*}}(\mathbf{x}) d\mathbf{x},$$

then we have

$$\begin{aligned} I_{22} &= \mathbb{E} \left[ \left| Z_{\boldsymbol{\theta}_*} \sum_{i=1}^m \frac{\theta_*^\zeta(i) \sum_{j=1}^k 1_{J(\mathbf{x}_j)=i}}{k} - Z_{\boldsymbol{\theta}_*} \int_{\mathcal{X}} \sum_{i=1}^m \theta_*^\zeta(i) 1_{J(\mathbf{x})=i} \varpi_{\tilde{\Psi}_{\boldsymbol{\theta}_*}}(\mathbf{x}) d\mathbf{x} \right| \right] \\ &= Z_{\boldsymbol{\theta}_*} \mathbb{E} \left[ \left| \frac{1}{k} \sum_{j=1}^k \left( \sum_{i=1}^m \theta_*^\zeta(i) 1_{J(\mathbf{x}_j)=i} \right) - \int_{\mathcal{X}} \left( \sum_{i=1}^m \theta_*^\zeta(i) 1_{J(\mathbf{x})=i} \right) \varpi_{\tilde{\Psi}_{\boldsymbol{\theta}_*}}(\mathbf{x}) d\mathbf{x} \right| \right] \quad (52) \\ &= O\left( \frac{1}{k\epsilon} + \sqrt{\epsilon} + \sqrt{\frac{\sum_{i=1}^k \omega_i}{k}} + \frac{1}{\sqrt{m}} + \sqrt{\sup_{\mathbf{x}} \text{Var}(\xi_n(\mathbf{x}))} \right), \end{aligned}$$

where the last equality follows from Lemma 12 as the step function  $\sum_{i=1}^m \theta_*^\zeta(i) 1_{J(\mathbf{x})=i}$  is bounded.

For  $I_3$ , by the boundedness of  $f$ , the mean value theorem and Cauchy-Schwarz inequality, we have

$$I_3 \lesssim \mathbb{E} \left[ \frac{1}{k} \sum_{i=1}^k \left| \theta_i^\zeta(J(\mathbf{x}_i)) - \theta_*^\zeta(J(\mathbf{x}_i)) \right| \right] \lesssim \frac{1}{k} \mathbb{E} \left[ \sum_{j=1}^k \sum_{i=1}^m \left| \theta_j(i) - \theta_*(i) \right| \right] \lesssim \frac{1}{k} \sqrt{\sum_{j=1}^k \mathbb{E} \left[ \|\boldsymbol{\theta}_j - \boldsymbol{\theta}_*\|^2 \right]}. \quad (53)$$

For the last term  $I_4$ , we first decompose  $\int_{\mathcal{X}} f(\mathbf{x})\pi(d\mathbf{x})$  into  $m$  disjoint regions to facilitate the analysis

$$\begin{aligned}\int_{\mathcal{X}} f(\mathbf{x})\pi(d\mathbf{x}) &= \int_{\cup_{j=1}^m \mathcal{X}_j} f(\mathbf{x})\pi(d\mathbf{x}) = \sum_{j=1}^m \int_{\mathcal{X}_j} \theta_{\star}^{\zeta}(j) f(\mathbf{x}) \frac{\pi(d\mathbf{x})}{\theta_{\star}^{\zeta}(j)} \\ &= Z_{\theta_{\star}} \int_{\mathcal{X}} \sum_{j=1}^m \theta_{\star}(j)^{\zeta} f(\mathbf{x}) 1_{J(\mathbf{x}_i)=j} \varpi_{\tilde{\Psi}_{\theta_{\star}}}(\mathbf{x})(d\mathbf{x}).\end{aligned}\tag{54}$$

Plugging (54) into the last term  $I_4$ , we have

$$\begin{aligned}I_4 &= \left| \mathbb{E} \left[ \frac{Z_{\theta_{\star}}}{k} \sum_{i=1}^k \sum_{j=1}^m \theta_{\star}(j)^{\zeta} f(\mathbf{x}_i) 1_{J(\mathbf{x}_i)=j} \right] - \int_{\mathcal{X}} f(\mathbf{x})\pi(d\mathbf{x}) \right| \\ &= Z_{\theta_{\star}} \left| \mathbb{E} \left[ \frac{1}{k} \sum_{i=1}^k \left( \sum_{j=1}^m \theta_{\star}^{\zeta}(j) f(\mathbf{x}_i) 1_{J(\mathbf{x}_i)=j} \right) \right] - \int_{\mathcal{X}} \left( \sum_{j=1}^m \theta_{\star}^{\zeta}(j) f(\mathbf{x}_i) 1_{J(\mathbf{x}_i)=j} \right) \varpi_{\tilde{\Psi}_{\theta_{\star}}}(\mathbf{x})(d\mathbf{x}) \right|.\end{aligned}\tag{55}$$

Applying the function  $\sum_{j=1}^m \theta_{\star}^{\zeta}(j) f(\mathbf{x}_i) 1_{J(\mathbf{x}_i)=j}$  to Lemma 12 yields

$$\left| \mathbb{E} \left[ \frac{1}{k} \sum_{i=1}^k f(\mathbf{x}_i) \right] - \int_{\mathcal{X}} f(\mathbf{x}) \varpi_{\tilde{\Psi}_{\theta_{\star}}}(\mathbf{x})(d\mathbf{x}) \right| = \mathcal{O} \left( \frac{1}{k\epsilon} + \sqrt{\epsilon} + \sqrt{\frac{\sum_{i=1}^k \omega_i}{k}} + \frac{1}{\sqrt{m}} + \sqrt{\sup_{\mathbf{x}} \text{Var}(\xi_n(\mathbf{x}))} \right).\tag{56}$$

Plugging (56) into (55) and combining  $I_1, I_{21}, I_{22}, I_3$  and Theorem 3, we have

$$\left| \mathbb{E} \left[ \frac{\sum_{i=1}^k \theta_i^{\zeta}(J_{\tilde{U}}(\mathbf{x}_i)) f(\mathbf{x}_i)}{\sum_{i=1}^k \theta_i^{\zeta}(J_{\tilde{U}}(\mathbf{x}_i))} \right] - \int_{\mathcal{X}} f(\mathbf{x})\pi(d\mathbf{x}) \right| = \mathcal{O} \left( \frac{1}{k\epsilon} + \sqrt{\epsilon} + \sqrt{\frac{\sum_{i=1}^k \omega_i}{k}} + \frac{1}{\sqrt{m}} + \sqrt{\sup_{\mathbf{x}} \text{Var}(\xi_n(\mathbf{x}))} \right),$$

which concludes the proof of the theorem.

## D More discussions on the algorithm

### D.1 An alternative numerical scheme

In addition to the numerical scheme used in (6) and (8) in the main body, we can also consider the following numerical scheme

$$\mathbf{x}_{k+1} = \mathbf{x}_k - \epsilon_{k+1} \frac{N}{n} \left[ 1 + \zeta\tau \frac{\log \theta_k(J_{\tilde{U}}(\mathbf{x}_k) \wedge m) - \log \theta_k(J_{\tilde{U}}(\mathbf{x}_k))}{\Delta u} \right] \nabla_{\mathbf{x}} \tilde{U}(\mathbf{x}_k) + \sqrt{2\tau\epsilon_{k+1}} \mathbf{w}_{k+1}.$$

Such a scheme leads to a similar theoretical result and a better treatment of  $\Psi_{\theta}(\cdot)$  for the subregions that contains stationary points.

### D.2 Bizarre peaks in the Gaussian mixture distribution

A bizarre peak always indicates that there is a stationary point of the same energy in somewhere of the sample space, as the sample space is partitioned according to the energy function in CSGLD. For example, we study a mixture distribution with asymmetric modes  $\pi(x) = 1/6N(-6, 1) + 5/6N(4, 1)$ . Figure 4 shows a bizarre peak at  $x$ . Although  $x$  is not a local minimum, it has the same energy as “-6” which is a local minimum. Note that in CSGLD,  $x$  and “-6” belongs to the same subregion.

### D.3 Simulations of multi-modal distributions

We run all the algorithms with 200,000 iterations and assume the energy and gradient follow the Gaussian distribution with a variance of 0.1. We include an additional quadratic regularizer  $(\|\mathbf{x}\|^2 - 7)1_{\|\mathbf{x}\|^2 > 7}$  to limit the samples to the center region. We use a constant learning rate 0.001 for SGLD,



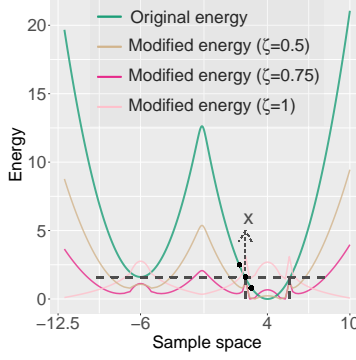


Figure 4: Explanation of bizarre peaks.

reSGLD, and CSGLD; We adopt the cyclic cosine learning rates with initial learning rate 0.005 and 20 cycles for cycSGLD. The temperature is fixed at 1 for all the algorithms, excluding the high-temperature process of reSGLD, which employs a temperature of 3. In particular for CSGLD, we choose the step size  $\omega_k = \min\{0.003, 10/(k^{0.8} + 100)\}$  for learning the latent vector. We fix 100 partitions and each energy bandwidth is set to 0.25. We choose  $\zeta = 0.75$ .

#### D.4 Extension to the scenarios with high- $\zeta$

In some complex big data experiments, the first subregion may dominate the probability mass and estimating  $\theta(i)$ 's for the high energy subregions can be quite difficult due to the limitation of floating points. If a small value of  $\zeta$  is used, the gradient multiplier  $1 + \zeta \tau \frac{\log \theta_*(i) - \log \theta_*((i-1) \vee 1)}{\Delta u}$  is close to 1 for any  $i$  and the algorithm will perform similarly to SGLD, except with different weights. When a large value of  $\zeta$  is used, the stochastic approximation update in Eq.(17) is slow **since  $\theta^\zeta$  is close to 0**. To tackle this issue, one solution is to include a high-order bias item in the stochastic approximation:

$$\theta_{k+1}(i) = \theta_k(i) + \omega_{k+1} \left( \theta_k^\zeta(J_{\bar{U}}(\mathbf{x}_{k+1}) + \omega_{k+1} 1_{i \geq J_{\bar{U}}(\mathbf{x}_{k+1})} \rho) \right) \left( 1_{i=J_{\bar{U}}(\mathbf{x}_{k+1})} - \theta_k(i) \right), \quad (57)$$

for  $i = 1, 2, \dots, m$ , where  $\rho$  is a constant. As shown early, our convergence theory allows inclusion of such a high-order bias term. In simulations, the high-order bias term  $\omega_{k+1}^2 1_{i \geq J_{\bar{U}}(\mathbf{x}_{k+1})} \rho$  penalized more on the higher energy regions, and thus accelerates the convergence in the early period.

In the computer vision examples, we set the momentum coefficient to 0.9 and the weight decay to 25. For CSGHMC and saCSGHMC, we set  $\omega_k = \frac{10}{k^{0.75} + 1000}$  and  $\rho = 1$  in (57) for both CIFAR10 and CIFAR100, and set  $\zeta = 1 \times 10^6$  for CIFAR10 and  $3 \times 10^6$  for CIFAR100.

**Can we make the algorithm more scalable:** The additional term  $\rho$  makes the algorithm less appealing in practice. To tackle that issue and make it more scalable to big datasets, we can adopt a more scalable and elegant stochastic approximation scheme proposed in Deng et al. [2022]

$$\theta_{k+1}(i) = \theta_k(i) + \omega_{k+1} \theta_k(J_{\bar{U}}(\mathbf{x}_{k+1}) \left( 1_{i=J_{\bar{U}}(\mathbf{x}_{k+1})} - \theta_k(i) \right).$$

Compared to Eq.(57), the dependence of  $\rho$  is no longer required. Moreover, since  $\theta(i) < 1$  for any  $i \in \{1, 2, \dots, m\}$ ,  $\theta(i)^\zeta \approx 0$  when  $\zeta \gg 1$ , which makes Eq.(57) hard to update. By contrast, the new scheme doesn't have this issue. Theoretically, a local stability shows that  $\theta_k(i)$  converges to a much smoother estimate  $(\int_{\mathcal{X}_i} \pi(\mathbf{x}) d\mathbf{x})^{\frac{1}{\zeta}}$  instead of the original  $\int_{\mathcal{X}_i} \pi(\mathbf{x}) d\mathbf{x}$  for  $i \in \{1, 2, \dots, m\}$  and  $\zeta > 1$ . Notably, the new target is proven to be easier to estimate for high-energy regions.

#### D.5 Number of partitions

A fine partition will lead to a smaller discretization error, but it may increase the risk in stability. In particular, it leads to large bouncy jumps around optima (a large negative learning rate, i.e.,  $\frac{\log \theta(2) - \log \theta(1)}{\Delta u} \ll 0$  in formula (8) may be caused there). Empirically, we suggest to partition the sample space into a moderate number of subregions, e.g. 10-1000, to balance between stability and discretization error.